JAEA-Research
2014-023

JAEA-Research

Study on Numerical Simulation of Bubble and Dissolved Gas Behavior in Liquid Metal Flow

Kei ITO, Masaaki TANAKA, Shuji OHNO and Hiroyuki OHSHIMA

Fast Reactor Computational Engineering Department
Advanced Fast Reactor Cycle System Research and Development Center
Sector of Fast Reactor Research and Development

November 2014

Japan Atomic Energy Agency

日本原子力研究開発機構

本レポートは独立行政法人日本原子力研究開発機構が不定期に発行する成果報告書です。
本レポートの入手並びに著作権利用に関するお問い合わせは、下記あてにお問い合わせ下さい。
なお、本レポートの全文は日本原子力研究開発機構ホームページ（http://www.jaea.go.jp）
より発信されています。

独立行政法人日本原子力研究開発機構 研究連携成果展開部 研究成果管理課
〒319-1195 茨城県那珂郡東海村白方白根2 番地4
電話 029-282-6387, Fax 029-282-5920, E-mail:ird-support@jaea.go.jp

This report is issued irregularly by Japan Atomic Energy Agency.
Inquiries about availability and/or copyright of this report should be addressed to
Institutional Repository Section,
Intellectual Resources Management and R&D Collaboration Department,
Japan Atomic Energy Agency.
2-4 Shirakata Shirane, Tokai-mura, Naka-gun, Ibaraki-ken 319-1195 Japan
Tel +81-29-282-6387, Fax +81-29-282-5920, E-mail:ird-support@jaea.go.jp

JAEA-Research 2014-023

Study on Numerical Simulation of Bubble and Dissolved Gas Behavior in Liquid Metal Flow

Kei ITO, Masaaki TANAKA, Shuji OHNO and Hiroyuki OHSHIMA

Fast Reactor Computational Engineering Department,
Advanced Fast Reactor Cycle System Research and Development Center,
Sector of Fast Reactor Research and Development,
Japan Atomic Energy Agency
Oarai-machi, Higashiibaraki-gun, Ibaraki-ken

(Received September 12, 2014)

In a sodium-cooled fast reactor, inert gas (bubbles or dissolved gas) exists in the primary coolant system. Such inert gas may cause disturbance in reactivity and/or degradation of IHX performance, and therefore, the inert gas behaviors have to be investigated to ensure the stable operation of a fast reactor. However, it is difficult to investigate the inert gas behaviors in liquid metal flows experimentally because measurement techniques applicable to opaque liquid are quite limited.

The Japan Atomic Energy Agency has developed a plant dynamics code SYRENA to simulate the concentration distributions of the dissolved gas and the bubbles in a fast reactor. In this study, the models in SYRENA code are improved to achieve accurate simulations, e.g. rigorous mole conservation of inert gas. Moreover, new models are introduced to simulate the various bubble behaviors in liquid metal flows. To validate the improved models and the newly developed models, the inert gas behaviors in the large-scale sodium-cooled reactor are simulated. As a result, it is confirmed that the complicated bubble dynamics in each component, e.g. core or IHX, can be simulated appropriately by SYRENA code.

Keywords: Fast Reactor, Inert Gas, Gas Bubble, Liquid Metal Flow, SYRENA

JAEA-Research 2014-023

液体金属流れ中における気泡･溶存ガス挙動の数値解析手法の研究

日本原子力研究開発機構 高速炉研究開発部門
次世代原高速炉サイクル研究開発センター　高速炉計算工学技術開発部
伊藤　啓、田中　正暁、大野　修司、大島　宏之

(2014 年 9 月 12 日　受理)

ナトリウム冷却高速炉の1次冷却系には､気泡もしくは溶存ガスの形態で不活性ガスが存在する。不活性ガスは、炉心反応度擾乱やIHX伝熱性能低下を引き起こす可能性があるため、高速炉の安定運転のためには不活性ガス挙動を調査する必要がある。しかし、不透明な液体金属中の不活性ガス挙動を実験的に調べることは困難であるため、日本原子力研究開発機構では、炉内における気泡・溶存ガス濃度分布を計算できるプラント挙動解析コードSYRENAを開発している。本研究では、SYRENAコード内で用いているモデルの高度化を行って解析精度の向上を図るとともに、様々な液体金属流れ場中の気泡挙動を解析するために必要となる新たなモデルの開発を行う。また、開発したモデルの検証としてナトリウム冷却大型高速炉の解析を行い、炉内の複雑な気泡挙動が計算できることを確認する。

大洗研究開発センター：〒311-1393　茨城県東茨城郡大洗町成田町 4002

Contents

目　次

List of tables

List of figures

This is a blank page.

1. Introduction

In the Japanese large-scale sodium-cooled fast reactor (JSFR), inert gas (bubbles or dissolved gas) is mixed in the primary coolant system due to cover gas (Ar) entrainment at free liquid level in the reactor upper plenum and bubble (He) released from control rods. Reactivity disturbance and decreased heat transfer performance in Intermediate Heat Exchanger (IHX) are concerned because of these bubbles or dissolved gas transported in primary coolant system, hence understanding bubbles and dissolved gas behavior in cooling system is important to ensure the stable operation of a fast reactor. The authors implement the development and verification of SYRENA code to evaluate the behavior of bubbles and dissolved gas in the primary coolant system of fast reactor. On the other hand, the inert gas exists in various liquid metal flows, e.g. the mercury target system which generates neutron by proton beam incident on mercury. Quantitative evaluation of the inert gas behaviors in such systems is inevitable to design configuration however observing bubble behavior in liquid metal flow is difficult, so bubble behavior evaluation using SYRENA code is considered effective.

In this study, the models in SYRENA code were improved to enhance accuracy of the analyses, and evaluation on the JSFR was implemented as the verification. In addition, new models were developed to apply SYRENA code to the evaluation of the inert gas behaviors in various liquid metal flow systems.

2. Brief Description of SYRENA Code

2.1 Inert Gas Behavior in Sodium-cooled Fast Reactor

Following is postulated as the source of inert gas contained in the primary coolant of the sodium cooled fast reactor.

- Ar cover gas dissolution from pressured free surface
- Ar cover gas entrainment at free surface
- Continuous He release generated at control rod
- Gas entrainment in an over flow area (depend on design of reactor vessel)

Also, following is postulated as bubbles or dissolved gas behavior in primary coolant system

- Bubble nucleation in the cooling area (IHX in fast reactor)
- Deposition/dissolution of inert gas at bubble surface (dissolution of bubble and deposition of dissolved gas)
- Bubble breakup (breakup of bubbles with a radius beyond the critical value)
- Transportation of bubble and dissolved gas by coolant flow
- Bubble release at free surface by buoyancy
- Bubble coalescence (can be ignored if no gas sump)

Hence, these phenomena must be modeled precisely to evaluate bubbles and dissolved gas behavior in sodium fast reactor.

2.2 Basic Formula of SYRENA Code

SYRENA code has been developed on the basis of VIBUL code[1)] which was developed in France to evaluate dissolved Ar behavior in sodium cooled fast reactor and was only intended for the Superphenix (SPX1) fast breeder reactor of France. In order to evaluate MONJU and JSFR, and to achieve collaborative analyses with other codes, drastic modifications have been implemented on whole VIBUL code such as program structure, phenomena model, discretization method, and analytical algorithm[2)]. As a result, SYRENA code uses multipoint approximation flow path model to analyze bubble number density in primary coolant system of fast reactor. Fundamental equations are the conservation equations of bubble mol count and dissolution mol count in a component. In those equations, bubbles are classified into i groups based on the bubble radius, and then bubble generation and collapse for each group are calculated. The fundamental equations of SYRENA code are shown below.

Conservation equation for bubble count in each component

$$V_{Na}\frac{d}{dt}N_{bi} = -\alpha_i V_{Na} N_{bi} - Q_{VNa} N_{bi} + Q_{VNae} N_{bie} + S_i \tag{2.1}$$

Note: V_{Na}: Plenum volume (m^3), N_{bi}: bubble number density of i groups, N_{mi}: mol count for each bubble in i groups, a_i: gas release coefficient of bubbles in i groups, Q_{VNa}: volumetric flow rate (m^3/s), S_i: source term. Subscript e indicates upstream volume factor (inflow).

Conservation equation for dissolved mol count in each component

$$V_{Na}\frac{d}{dt}N_d = -D\ \left(N_d - H\quad p_{libre}\right) -\ Q_{VNa}N_d + Q_{VNae}N_{de} - V_{Na}\sum N_{bi}\frac{d}{dt}N_{mi} \qquad (2.2)$$

Note: N_d: dissolved mol concentration, H: Henry's constant, P_{libre}: cover gas pressure (Pa), and D: effective diffusion coefficient determined by free surface liquid velocity.

3. Improvement of Models in SYRENA Code

3.1 Explicit Discretization of Bubble Mole Conservation Equation

SYRENA code uses the conservation equation for bubble count and dissolved mol count to calculate bubble number density N_b, bubble mol count N_{mi} and dissolved mol concentration N_d. This calculation is completed originally with an implicit method however malfunction of algorithm of implicit method (problem with bubble count determination) inhibits the strict conservations of bubble mol count and dissolved mol count inside the system. Thus, the fundamental equations are discretized explicitly (explicit method) to establish analytical algorithm satisfying the mol conservation.

Conservation equations for bubble mol count and dissolved mol count are shown in equations 2.1 and 2.2. Moreover, gas transport between bubble and sodium is shown in the equation below.

$$\frac{dN_{mi}}{dt} = -\,k\,4\pi\,r_i^2\,\left[N'_d - N_d\right] \tag{3.1}$$

Note: k: gas transport coefficient between bubble and sodium, r_i: representative radius of bubbles in group i, N'_d: molar solubility. Explicit discretization is applied to the equations 2.1, 3.1 and 2.2 to obtain the following equations 3.2, 3.4 and 3.6, respectively. In those equations, superscripts n and n+1 indicate the time.

Bubble number density N_b

$$V_{Na}\frac{{N_{bi}}^{n+1} - {N_{bi}}^{n}}{\Delta t} = -\alpha_i V_{Na}{N_{bi}}^{n} - Q_{VNa}{N_{bi}}^{n} + Q_{VNae}{N_{bie}}^{n} \tag{3.2}$$

$${N_{bi}}^{n+1} = \frac{\Delta t(-\alpha_i V_{Na}{N_{bi}}^{n} - Q_{VNa}{N_{bi}}^{n} + Q_{VNae}{N_{bie}}^{n}) + V_{Na}{N_{bi}}^{n}}{V_{Na}} \tag{3.3}$$

Mol count for each bubble class N_{mi}

$$\frac{{N_m}^{n+1} - {N_m}^{n}}{\Delta t} = -\;\;k\;\;4\pi\;\;(r_i^n)^2\;\;\left[N'_d - {N_d}^{n}\right] \tag{3.4}$$

$${N_{mi}}^{n+1} = -\,k\,4\pi\,(r_i^n)^2\left[N'_d - {N_d}^{n}\right]\Delta t + {N_{mi}}^{n} \tag{3.5}$$

Dissolved mol concentration N_d

$$V_{Na}\frac{{N_d}^{n+1}-{N_d}^{n}}{\Delta t}=-D\left({N_d}^{n}-H\ p_{libre}\right)-Q_{VNa}{N_d}^{n}+Q_{VNae}{N_{de}}^{n}-V_{Na}\sum N_{bi}^{n+1}\frac{d}{dt}N_{mi} \tag{3.6}$$

$${N_d}^{n+1}=\left[-D\left({N_d}^{n}-H\ p_{libre}\right)-Q_{VNa}{N_d}^{n}+Q_{VNae}{N_{de}}^{n}-V_{Na}\sum N_{bi}^{n+1}\frac{d}{dt}N_{mi}\right]\cdot\frac{\Delta t}{V_{Na}}+{N_d}^{n} \tag{3.7}$$

Note: the temporal differentiation term at the right side of the equation 3.6 is calculated by substituting the equation 3.4.

3.2 Initialization of Calculation Array for Nucleation

Volume of bubbles generated due to the nucleation in IHX is stored in the array nb_nu(), however initialization of the array has not been done originally in SYRENA code. Thus, even in the condition unsatisfying the nucleation generation, bubble generation could be calculated. To prevent this error, initialization of nb_nu() is added.

3.3 Examination on Saturated Temperature Calculation of Inert Gas in Sodium

The equation below is used to calculate saturated temperature of gas T_{sat} in sodium when calculating nucleation in IHX.

$$T_{sat}=\frac{-4542}{\log\left(\frac{M_{Na}N_{de}}{P_L\rho_{Na}}\right)+2.13} \tag{3.8}$$

Note: M_{Na}: molar mass in coolant sodium, N_{de}: dissolved mol concentration at IHX inlet, P_L: fluid pressure、ρ_{Na}: sodium concentration. It is determined that nucleation is generated if $T_{sat} > T_s$, in VIBUL. However, T_s is outlet temperature of sodium in IHX. Since volumetric flow rate and dissolved mol concentration vary with temperature change in IHX, IHX inlet value should be used for the calculation of ρ_{Na} to handle the equation 3.8 accurately. Originally, the dissolved mol concentration at IHX inlet is used in the calculation even though the density at the calculation point in the IHX is used as ρ_{Na}. Therefore, the saturated temperature of sodium is not calculated accurately. As a consequence, the nucleation may not occur even in the condition it should occur, and temporal fluctuation is seen for the volume of bubble generation as shown in Fig 3.1 (and Fig. 3.2). To resolve this problem, SYRENA code is modified to use the sodium density at IHX inlet as ρ_{Na}. As a result, the temporal fluctuation for the volume of bubble generation is inhibited as shown in Fig. 3.3 (and Fig. 3.4).

3.4 Derivation of Appropriate Pressure Calculation in IHX

In the IHX, bubble generation (reduction of the dissolved mol concentration) by the nucleation is calculated using the equation below.

$$\begin{aligned}\Delta N_d &= Q_{VNae} N_{de} - Q_{VNa}\, N_{dsat} \\ &= Q_{VNae} N_{de} - Q_{VNa}\,(H_s . P_s)\end{aligned} \tag{3.9}$$

Originally, the outlet pressure is calculated as $P_s = P_0 + \rho_{Na} g h$ without consideration of pressure loss in IHX. Here, P_0 is cover gas pressure and h is IHX height. Hence, dissolved mol concentration (molar solubility) at the IHX outlet and also generated bubble diameter may not be calculated accurately because they are sensitive to pressure. Therefore, the pressure calculation is improved to use the fluid pressure P_L in the equation below to calculate gas saturated temperature in sodium to consider influence of pressure loss P_{loss}.

$$P_L = P_0 + \rho_{Na} g h - P_{loss} \tag{3.10}$$

Pressure loss is hypothetically consistent throughout IHX in calculating pressure at a point in IHX.

3.5 Correction of Dissolved Mol Concentration Calculation at Mixing Point

The bubble number density N_{bi_out} and dissolved mol concentration N_{d_out} in the outflow at a mixing point are calculated originally as below.

$$N_{bi\_out} = \frac{\Sigma Q_{in}(k) N_{bi\_in}(k)}{\Sigma Q_{in}(k)} \tag{3.11}$$

$$N_{d\_out} = \frac{\Sigma Q_{in}(k) N_{d\_in}(k)}{\Sigma Q_{in}(k)} \tag{3.12}$$

Here, Q_{in} 、N_{bi_in} 、N_{d_in} are flow rate, bubble number density and dissolved mol concentration of each inflow pass at the mixing point, respectively and k is the index number of the each flow path. The equations 3.11 and 3.12 use total inflow at the joint $\Sigma Q_{in}(k)$ for the calculation, however if the inflow temperatures are different, the outlet (mixed) flow rate is not the same as the total inlet flow rate. In such cases, the molar conservation of bubble and dissolved gas is not satisfied. Thus the equations 3.11 and 3.12 are modified as below.

$$N_{bi\_out} = \frac{\Sigma Q_{in}(k) N_{bi\_in}(k)}{Q_{out}} \tag{3.13}$$

$$N_{d\_out} = \frac{\Sigma Q_{in}(k) N_{d\_in}(k)}{Q_{out}} \tag{3.14}$$

Note: Q_{out} is total outlet flow rate at the mixing point and calculated as below.

$$Q_{out} = \frac{\Sigma \rho_{Na}(k) Q_{VNae}(k)}{\rho'_{Na}} \tag{3.15}$$

Note: $\rho_{Na}(k)$ is the density of inflow at each flow path, and ρ'_{Na} is the coolant density of outflow at the mixing point.

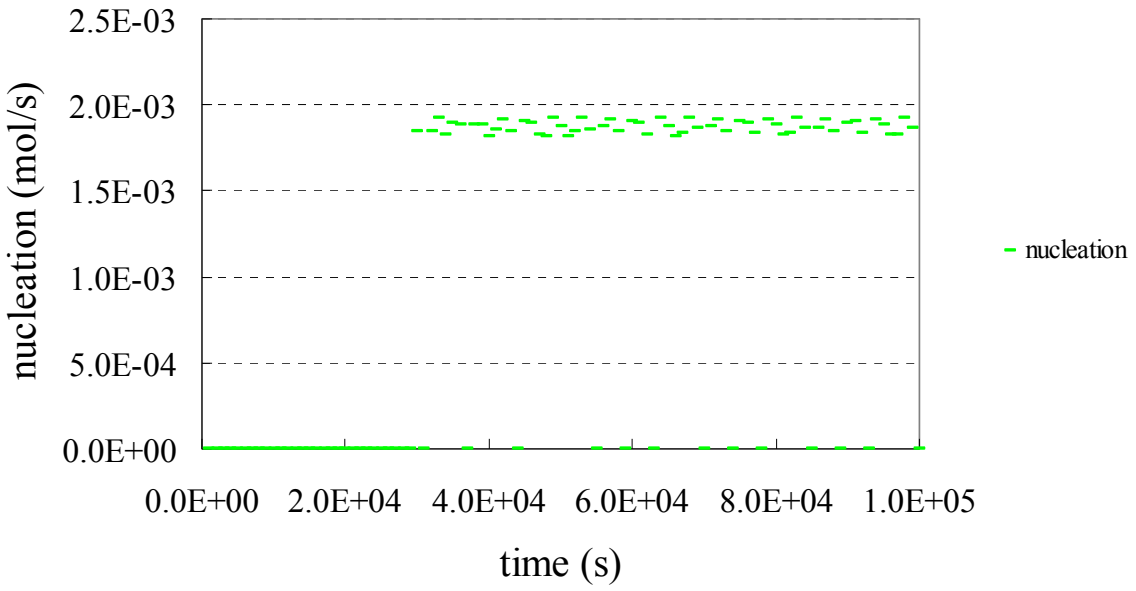

Fig.3.1 Bubble generation (nucleation) in IHX (before model improvement)

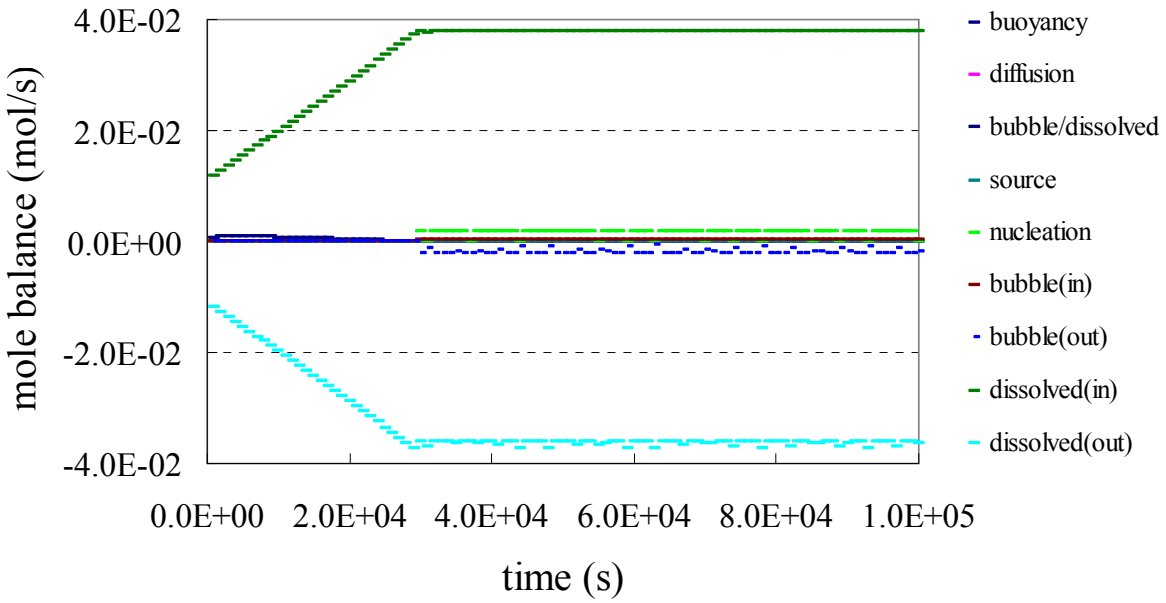

Fig.3.2 Molar balance in IHX (before model improvement)

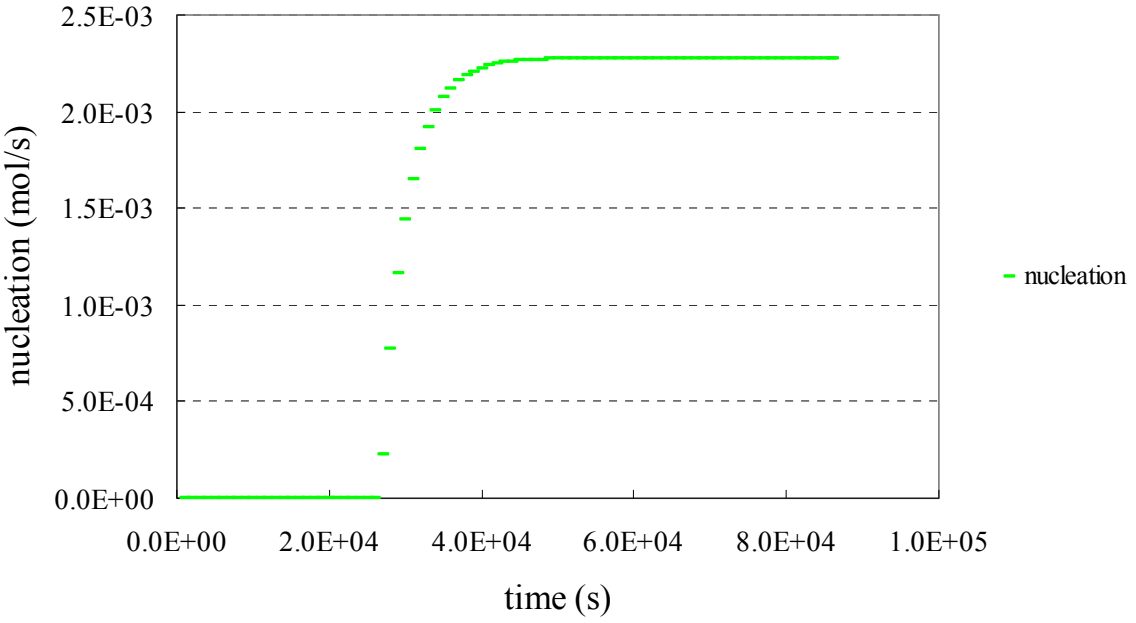

Fig.3.3 Bubble generation (nucleation) in IHX (after model improvement)

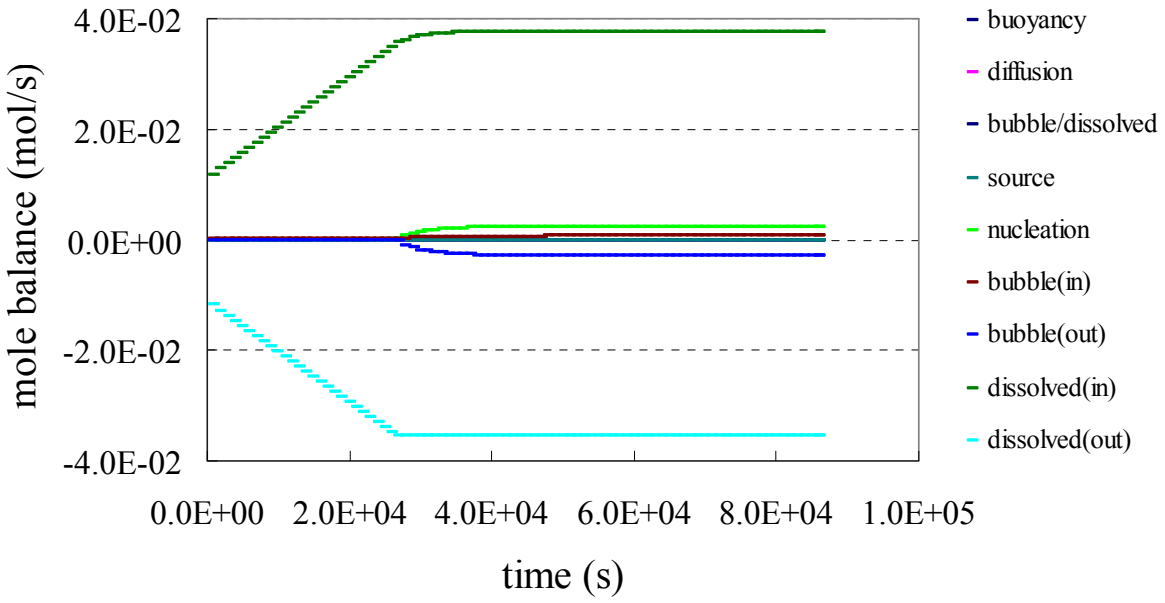

Fig.3.4 Mole balance in IHX (after model improvement)

4. Simulation of Inert Gas Behavior in Sodium-cooled Fast Reactor

To verify the improved models in SYRENA code, bubble/ dissolved gas behavior in the primary coolant system of sodium cooled fast reactor is evaluated. Note that in addition to the improvement shown in chapter three, SYRENA code here uses an accurate evaluation approach for the bubble behavior in the upper plenum region[3] (based on three dimensional numerical simulation, release ratio of the inflow bubble from the reactor core to the cover gas region, outflow ratio to the hot leg pipe, and dissolved ratio into the coolant are modeled as the correlating formula with dimensionless parameters). Furthermore, bubble generation/ separation model at the heat exchanging surface of IHX[4], in which the balance of surface tension, growing force and lift force is considered to provide the bubble separation condition, are adopted.

4.1 Simulation Condition

In this report, bubble/ dissolved gas behavior in normal operating condition in sodium cooled fast reactor system is simulated. The unsteady calculation is from initiating condition with "0" bubble and dissolved gas in all the components to the steady state when the temporal variations become sufficiently small.

Simulation cases

Inert gas generation volume and inert gas types (Ar, He) are used as the parameters to simulate four cases in table 4.1. Case-Ar(1/10) and Case-He(1/10) are the simulation cases with one tenth bubble source of those in Case-Ar-ref and Case-He-ref, respectively.

Simulation model

The simulation model is constructed based on the primary cooling system of sodium cool fast reactor as shown in Fig. 4.1. This model consists of 1) upper plenum, 2) hot leg piping, 3) IHX, 4) pump, 5) cold leg piping, 6) lower plenum, 7) core bypath, 8) core. Liquid sodium, the coolant is released from the reactor vessel and goes through hot leg piping (1-pipe x 2-loops), integrated pump-IHX, cold leg piping (2-pipes x 2-loop) then return to the reactor vessel. Source of the inert gas mixed in the coolant considers entrained Ar gas and the dissolution at free surface of the upper plenum and He bubble release from the control rod (B4C).

4.2 Simulation Result

Based on the simulation results, molar balance in each component, distribution of bubble number density in each evaluation point and the calculated void fraction are studied.

Ar gas behavior

Molar balance in each component, distribution of bubble number density at each calculation

poins, void fraction in each component, nucleation parameter in IHX are shown in table 4.2 and 4.3, Fig. 4.2and 4.3, table 4.6, and table 4.7 respectively.

In the upper plenum, the dissolved mol count rapidly increases due to the bubble dissolution. On the other hand, at the IHX outlet, bubble mol count reaches the maximum value while dissolved mol count being the smallest value due to the deposition of dissolved gas as bubbles. Diameter of the bubbles generated in the IHX decreases due to the pressure rise in the pump. At the downstream of the pump, the diameter increases gradually due to the gradual pressure decrease. In the core, sodium solubility increases due to the coolant temperature rise hence bubble mol count decreases and dissolved mol count increases.

To investigate the influence on Ar gas behavior from bubble source, simulation results of Case-Ar-ref and Case-Ar(1/10) are compared. Since they both share same conditions of coolant flow, temperature, and pressure, no significant difference in bubble diameter distribution is seen in each component. Also, dissolved mol counts of inflow and outflow in each component between IHX outlet to upper plenum inlet substantially coincides. Difference in bubble source influences distribution of bubble number density and the void fraction; they are proportional to bubble source, that is, the bubble number density and the void fraction in Case-Ar(1/10) are about one tenth of those in Case-Ar-ref.

He gas behavior

Molar balance in each component, distribution of bubble number density at each evaluation point, void fraction in each component, and nucleation parameter in IHX are shown in table 4.4 and 4.5, Fig. 4.4 and 4.5, table 4.8, and table 4.9 respectively.

He gas bubble source from control rod released in core gradually dissolves in coolant in the core and upper plenum. At the IHX outlet, the bubble mol count is the maximum value while the dissolved mol count being the smallest value due to the deposition of the dissolved gas as bubbles. The bubbles generated in IHX loose the diameter due to pressure rise in the pump and at the downstream of the pump, gradually gain the diameter due to gradual pressure drop.

Simulation results of Case-He-ref and Case-He(1/10) are compared to study the influence of bubble source on He gas behavior. Both share all the condition except for bubble source, no significant difference is seen in the distribution of bubble diameter. Also, inflow and outflow dissolved mol count in each component substantially coincide. As a result bubble source difference only influence the distribution of bubble number density and the calculated void fracture, they becomes about one tenth of those in Case-He(1/10), proportional to bubble source.

Comparison of Ar gas behavior and He gas behavior

Behaviors of Ar gas and He gas are compared in the same simulation models and the bubble source condition (e.g. Case-Ar-ref and Case-He-ref). Solubility of Ar gas to sodium is smaller than that of He gas, and therefore, dissolved mol count of Ar gas in each component is about one order smaller than that of He gas. Contrary, Ar gas bubble source is larger than that of He gas so bubble mol count of

Ar gas in each component is about one order larger. However, when comparing bubble/dissolved gas in primary coolant system, they match qualitatively in tendencies of bubble deposition in IHX and bubble dissolution in core and upper plenum.

These simulation results represent bubble/dissolved gas behaviors in primary coolant system of fast reactor qualitatively correct to conclude evaluation using SYRENA code is valid.

Table 4.1 Simulation condition for bubble and dissolved gas behavior in fast reactor

Case	Inert Gas	Gas Source (mol/s)
Case-Ar-ref	Ar	1.7×10^{-4}
Case-Ar(1/10)	Ar	1.7×10^{-5}
Case-He-ref	He	1.08×10^{-5}
Case-He(1/10)	He	1.08×10^{-6}

Table 4.2 Molar balance (mol/s) of Ar gas in Case-Ar-ref

Component	Buoyant release	Interfacial dissolution	Bubble dissolution	Bubble source	Nucleation	Inlet bubble mole count	Outlet bubble mole count	Inlet dissolved mol count	Outlet dissolved mol count
①Upper Plenum	-1.65E-03	3.16E-06	-1.29E-03	1.70E-03	0.00E+00	1.30E-02	-1.17E-02	1.62E-03	-2.91E-03
②Hot Leg Pipe	0.00E+00	0.00E+00	-5.10E-05	0.00E+00	0.00E+00	1.17E-02	-1.17E-02	2.91E-03	-2.97E-03
③IHX	0.00E+00	0.00E+00	-2.36E-06	0.00E+00	1.79E-03	1.17E-02	-1.35E-02	2.97E-03	-1.17E-03
④Pump	-4.82E-05	-1.04E-09	-8.91E-06	0.00E+00	0.00E+00	1.35E-02	-1.34E-02	1.17E-03	-1.18E-03
⑤Cold Leg Pipe	0.00E+00	0.00E+00	-2.19E-06	0.00E+00	0.00E+00	1.34E-02	-1.34E-02	1.18E-03	-1.18E-03
⑥Lower Plenum	0.00E+00	0.00E+00	-5.35E-05	0.00E+00	0.00E+00	1.34E-02	-1.33E-02	1.18E-03	-1.24E-03
⑦Core	0.00E+00	0.00E+00	-3.85E-04	0.00E+00	0.00E+00	1.32E-02	-1.28E-02	1.22E-03	-1.61E-03
⑧Core Bypass	0.00E+00	0.00E+00	-1.91E-06	0.00E+00	0.00E+00	1.48E-04	-1.46E-04	1.37E-05	-1.57E-05

Table 4.3 Molar balance (mol/s) of Ar gas in Case-Ar(1/10)

Component	Buoyant release	Interfacial dissolution	Bubble dissolution	Bubble source	Nucleation	Inlet bubble mole count	Outlet bubble mole count	Inlet dissolved mol count	Outlet dissolved mol count
①Upper Plenum	-1.68E-04	3.42E-06	-1.53E-04	1.70E-04	0.00E+00	1.41E-03	-1.26E-03	1.23E-03	-1.39E-03
②Hot Leg Pipe	0.00E+00	0.00E+00	-6.21E-06	0.00E+00	0.00E+00	1.26E-03	-1.25E-03	1.39E-03	-1.40E-03
③IHX	0.00E+00	0.00E+00	-3.92E-07	0.00E+00	2.15E-04	1.25E-03	-1.47E-03	1.40E-03	-1.18E-03
④Pump	-4.94E-06	-1.00E-09	-1.03E-06	0.00E+00	0.00E+00	1.47E-03	-1.46E-03	1.18E-03	-1.18E-03
⑤Cold Leg Pipe	0.00E+00	0.00E+00	-2.54E-07	0.00E+00	0.00E+00	1.46E-03	-1.46E-03	1.18E-03	-1.18E-03
⑥Lower Plenum	0.00E+00	0.00E+00	-6.38E-06	0.00E+00	0.00E+00	1.46E-03	-1.46E-03	1.18E-03	-1.19E-03
⑦Core	0.00E+00	0.00E+00	-4.42E-05	0.00E+00	0.00E+00	1.44E-03	-1.40E-03	1.17E-03	-1.22E-03
⑧Core Bypass	0.00E+00	0.00E+00	-7.01E-07	0.00E+00	0.00E+00	1.62E-05	-1.55E-05	1.32E-05	-1.39E-05

Table 4.4 Molar balance (mol/s) of He gas in Case-He-ref

Component	Buoyant release	Interfacial dissolution	Bubble dissolution	Bubble source	Nucleation	Inlet bubble mole count	Outlet bubble mole count	Inlet dissolved mol count	Outlet dissolved mol count
①Upper Plenum	-9.54E-05	0.00E+00	-7.75E-04	0.00E+00	0.00E+00	1.41E-03	-5.41E-04	4.28E-02	-4.36E-02
②Hot Leg Pipe	0.00E+00	0.00E+00	-2.88E-05	0.00E+00	0.00E+00	5.41E-04	-5.12E-04	4.36E-02	-4.36E-02
③IHX	0.00E+00	0.00E+00	-3.67E-04	0.00E+00	1.57E-03	5.12E-04	-2.14E-03	4.36E-02	-4.20E-02
④Pump	-1.20E-05	-4.51E-08	-4.79E-05	0.00E+00	0.00E+00	2.14E-03	-2.08E-03	4.20E-02	-4.21E-02
⑤Cold Leg Pipe	0.00E+00	0.00E+00	-1.19E-05	0.00E+00	0.00E+00	2.08E-03	-2.07E-03	4.21E-02	-4.21E-02
⑥Lower Plenum	0.00E+00	0.00E+00	-2.72E-04	0.00E+00	0.00E+00	2.07E-03	-1.79E-03	4.21E-02	-4.23E-02
⑦Core	0.00E+00	0.00E+00	-4.77E-04	1.08E-04	0.00E+00	1.77E-03	-1.41E-03	4.19E-02	-4.23E-02
⑧Core Bypass	0.00E+00	0.00E+00	-1.35E-05	0.00E+00	0.00E+00	1.99E-05	-6.49E-06	4.70E-04	-4.84E-04

Table 4.5 Molar balance (mol/s) of He gas in Case-He(1/10)

Component	Buoyant release	Interfacial dissolution	Bubble dissolution	Bubble source	Nucleation	Inlet bubble mole count	Outlet bubble mole count	Inlet dissolved mol count	Outlet dissolved mol count
①Upper Plenum	-9.00E-06	0.00E+00	-7.39E-05	0.00E+00	0.00E+00	1.34E-04	-5.12E-05	4.21E-02	-4.22E-02
②Hot Leg Pipe	0.00E+00	0.00E+00	-2.75E-06	0.00E+00	0.00E+00	5.12E-05	-4.83E-05	4.22E-02	-4.22E-02
③IHX	0.00E+00	0.00E+00	-3.53E-05	0.00E+00	1.50E-04	4.83E-05	-2.04E-04	4.22E-02	-4.21E-02
④Pump	-1.14E-06	-4.57E-08	-4.56E-06	0.00E+00	0.00E+00	2.04E-04	-1.98E-04	4.21E-02	-4.21E-02
⑤Cold Leg Pipe	0.00E+00	0.00E+00	-1.14E-06	0.00E+00	0.00E+00	1.98E-04	-1.97E-04	4.21E-02	-4.21E-02
⑥Lower Plenum	0.00E+00	0.00E+00	-2.60E-05	0.00E+00	0.00E+00	1.97E-04	-1.71E-04	4.21E-02	-4.21E-02
⑦Core	0.00E+00	0.00E+00	-4.56E-05	1.08E-05	0.00E+00	1.69E-04	-1.34E-04	4.16E-02	-4.17E-02
⑧Core Bypass	0.00E+00	0.00E+00	-1.34E-06	0.00E+00	0.00E+00	1.90E-06	-5.57E-07	4.68E-04	-4.69E-04

Table 4.6 Ar gas void fraction in each component

Component	Case-Ar-ref	Case3-Ar(1/10)
①Upper Plenum	2.41E-05	2.59E-06
②Hot Leg Pipe	2.40E-05	2.58E-06
③IHX	2.89E-05	3.16E-06
④Pump	2.88E-05	3.14E-06
⑤Cold Leg Pipe	2.88E-05	3.14E-06
⑥Lower Plenum	2.87E-05	3.13E-06
⑦Core	2.66E-05	2.90E-06
⑧Core Bypass	2.83E-05	2.99E-06

Table 4.7 Ar gas nucleation parameter

Case	Nucleation Height (m)	Minimum Nucleation Bubble Radius (m)	Maximum Nucleation Bubble Radius (m)
Case-Ar-ref	1.73	4.78E-05	5.56E-05
Case-Ar(1/10)	0.295	4.78E-05	5.14E-05

Table 4.8 He gas void fraction in each component

Component	Case-He-ref	Case3-He(1/10)
①Upper Plenum	1.04E-06	9.79E-08
②Hot Leg Pipe	9.80E-07	9.25E-08
③IHX	4.28E-06	4.07E-07
④Pump	4.16E-06	3.96E-07
⑤Cold Leg Pipe	4.13E-06	3.93E-07
⑥Lower Plenum	3.59E-06	3.41E-07
⑦Core	2.72E-06	2.59E-07
⑧Core Bypass	1.17E-06	1.00E-07

Table 4.9 He gas nucleation parameter

Case	Nucleation Height (m)	Minimum Nucleation Bubble Radius (m)	Maximum Nucleation Bubble Radius (m)
Case-He-ref	0.115	6.63E-05	7.27E-05
Case-He(1/10)	0.011	6.63E-05	7.22E-05

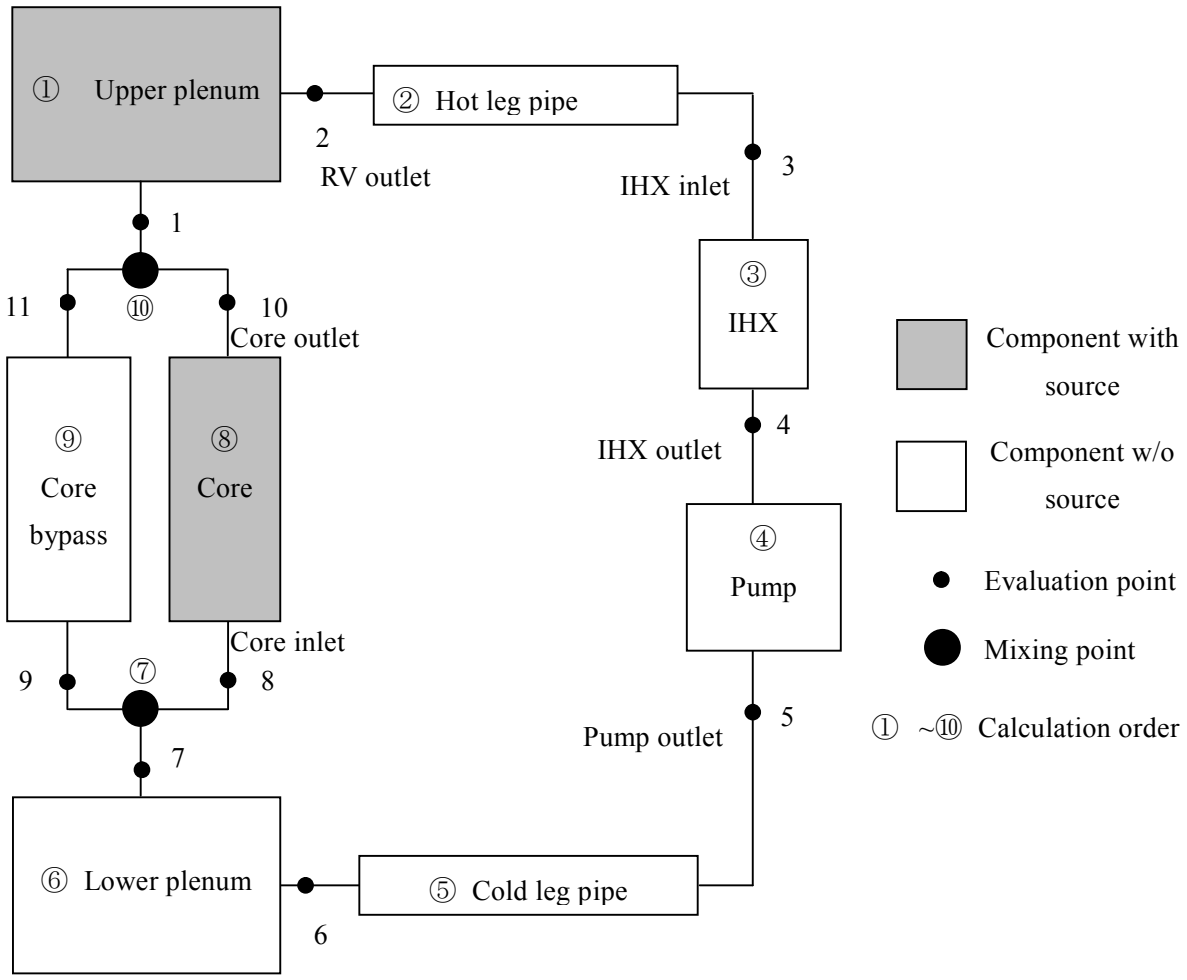

Fig.4.1 Simulation model of bubble/ dissolved gas behavior in fast reactor

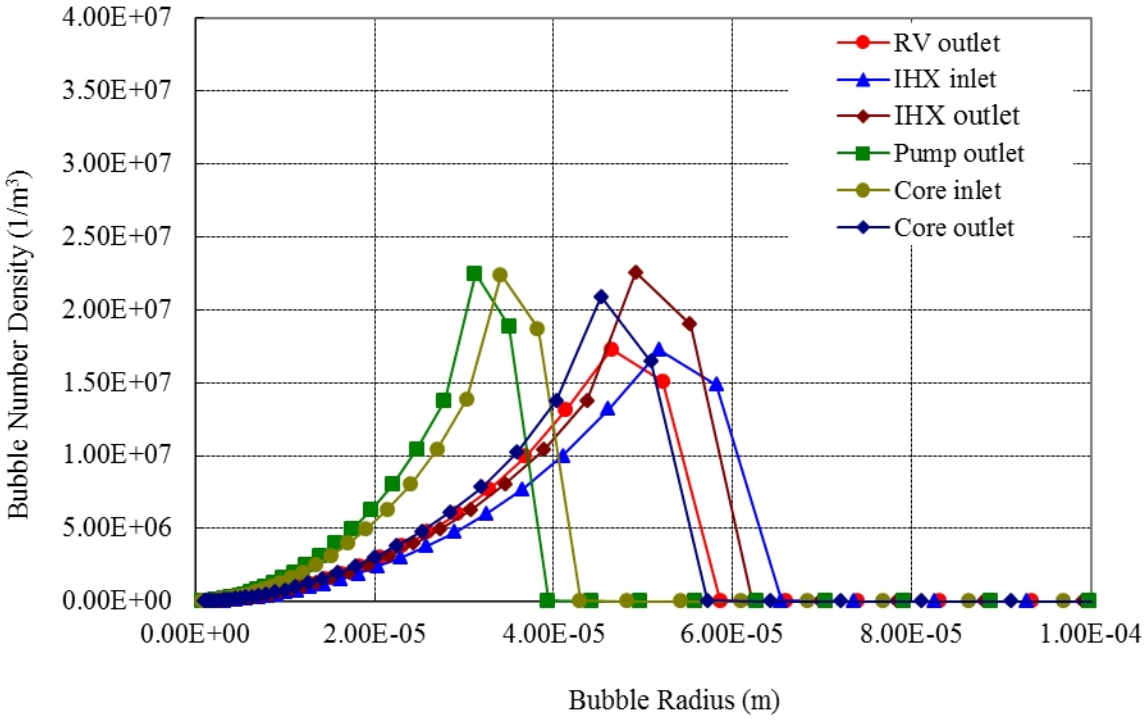

Fig.4.2 Distribution of bubble number density of Ar gas in Case-Ar-ref

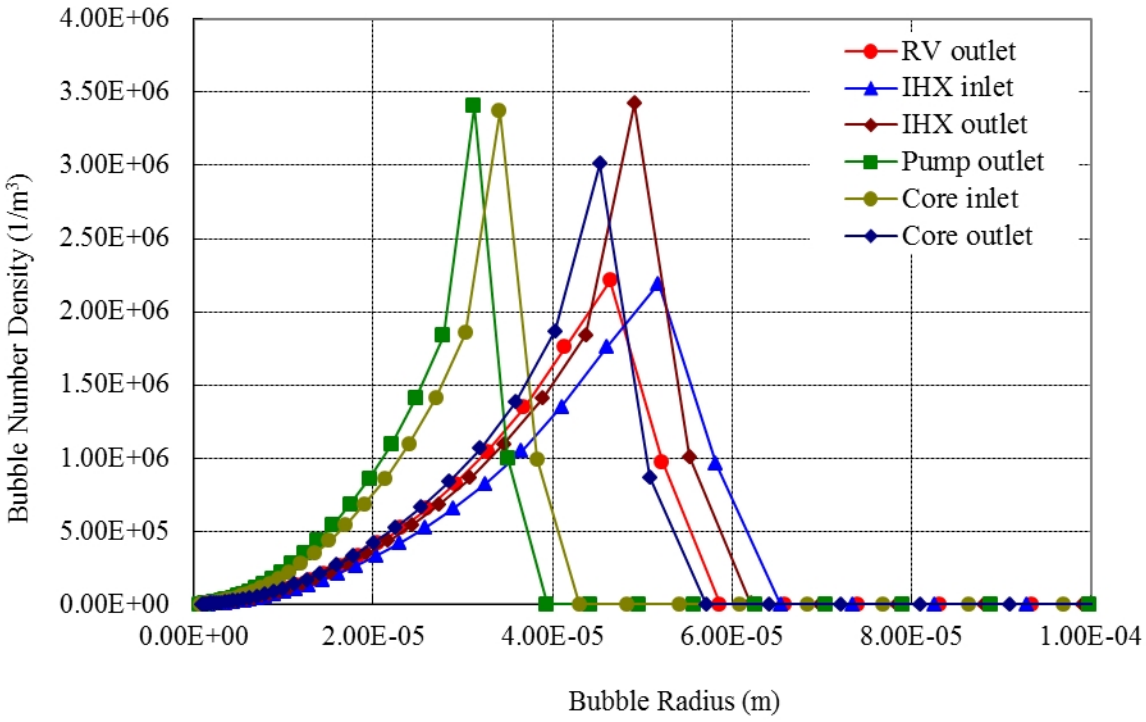

Fig.4.3 Distribution of bubble number density of Ar gas in Case-Ar(1/10)

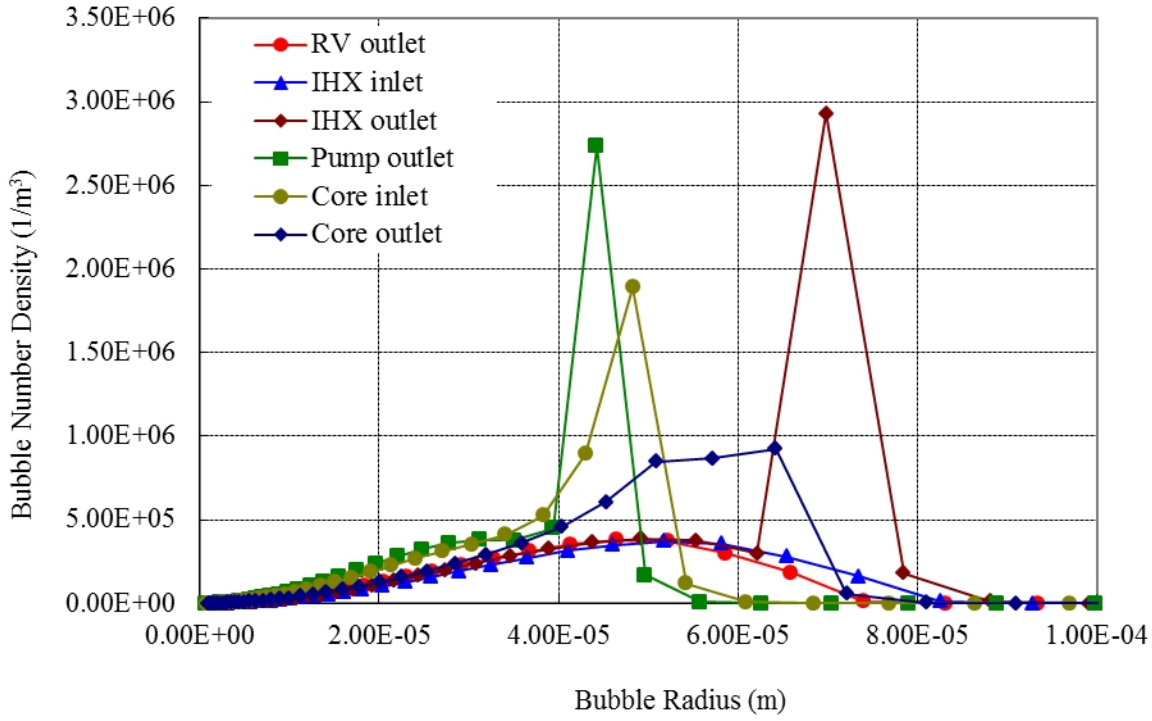

Fig.4.4 Distribution of bubble number density of He gas in Case-He-ref

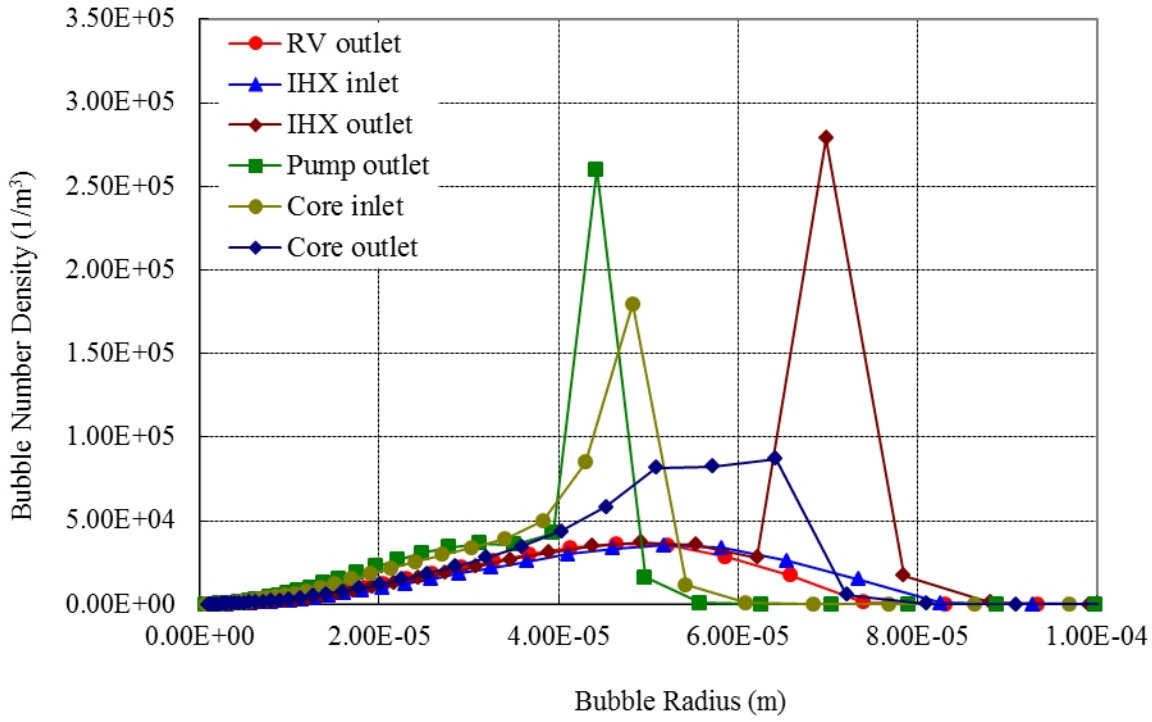

Fig.4.5 Distribution of bubble number density of He gas in Case-He(1/10)

5. Model Development for Simulation of Various Liquid Metal Flows

In this chapter new models are developed to evaluate the inert gas behaviors in various liquid metal flows using SYRENA code.

5.1 Introduction of Physical Property Function

To evaluate mercury systems, physical property values of mercury are introduced to SYRENA code as the functions of temperature T by polynomial approximation of the discrete values in literature[5].

Density ρ

$$\rho = 5.85714285714189\times10^{-4}\cdot T^2 - 2.83071428571419\cdot T + 1.43235714285714\times10^{4} \quad (5.1)$$

Viscosity coefficient η

$$\eta = 7.27272727276616\times10^{-14}\cdot T^4 - 1.51919191919784\times10^{-10}\cdot T^3 + 1.21696969697336\times10^{-7}\cdot T^2 - 4.52180375181325\times10^{-5}\cdot T + 7.64757575758196\times10^{-3} \quad (5.2)$$

Surface tension σ

$$\sigma = -1.06666666665376\times10^{-13}\cdot T^5 + 2.13939393942393\times10^{-10}\cdot T^4 - 1.68303030312010\times10^{-7}\cdot T^3 + 6.45863636420736\times10^{-5}\cdot T^2 - 1.22364545467927\times10^{-2}\cdot T + 1.39866233778113 \quad (5.3)$$

Helium solubility 3.89×10^{-7} (mol-He/mol-Hg) at 0.1 (MPa), 300 (K) from literature[6] is used without considering the dependence on temperature since existence of temperature-dependent solubility data is uncertain. Moreover, diffusion coefficient D (m^2/s) is calculated by the Stokes-Einstein equation below.

$$D = \frac{RT}{N6\pi\eta r_g} \quad (5.4)$$

Note: R is the gas constant = 8.3144 (J/mol*K), N is the Avogadro number (= 6.02×10^{23}), r_g is particle radius of gas (m), which is 0.93×10^{-10} (m) for Helium atom[7].

5.2 Extension to Open-loop System

Since SYRENA code is developed for the simulations of closed loop systems (such as JSFR), it is not applicable to an open loop system. In this report, an open loop model is developed.

Bubble number density and dissolved mol concentration in each component refer to the outflow value from their upstream components since liquid circulate inside the loop in a closed system. On the other hand liquid does not circulate in an open loop system hence inflow value in first component cannot be calculated. Hence, SYRENA code is modified to refer to the input values as the inflow data at the first component. Three variables (iflgoplp: selection of open/close loop, nbinp and ndinp: dissolved mol concentration and bubble number density of each bubble class flowing into the first component in open loop) are added for this modification.

5.3 Development of Large Bubble Release Model

In some liquid metal flow systems, a degassing device, e.g. vertical tube, is installed to release large bubbles. Bubble release phenomenon from the vertical tube is shown in Fig. 5.1. It is postulated that large bubbles receives the influence of buoyancy force to be released outside the pipe through the degassing tube before reaching pipe outlet. On the other hand, small bubbles have smaller buoyancy force so it is postulated to be transported to the pipe outlet.

To model large bubble release, the bubble number density is set to "0" when the bubble diameter is larger than the specified input value. This process of making bubble number density "0" is implemented after bubble redistribution and bubble breakup processes. Two variables (iflgbubrel: selection of model, rrel: minimum radius of released bubble) are introduced as new input.

As verification of large bubble release model, SYRENA simulation is implemented by arranging two components parallel, injecting bubbles in upstream component and activating the large bubble release model in downstream component. Main simulation conditions are shown below.

Component volume : 1.0 (m^3)
Component temperature : 20 (^oC)
Pressure : 1.0×10^5 (Pa)
Fluid : water
Gas : air
Flux : 10 (kg/s)
Loop type : open loop

Five simulations with rrel = ∞ (w/o large bubble release model), 3.5×10^{-3}, 3.0×10^{-3}, 2.5×10^{-3}, 2.0×10^{-3} (m), are implemented. Simulation results are shown in Fig. 5.2. In every case, bubble number density exceeding the specified release radius is being "0" showing that large bubble release model functions correctly.

5.4 Modeling of Bubble Release in Surge Tank

A surgetank is installed to remove bubbles in some liquid metal flow systems. An example of the surgetank is shown in Fig. 5.3. In this surge tank, bubbles are released by buoyancy force. Moreover, elbow pipe at the surgetank inlet creates swirl flow in the surgetank so the duration of the bubble staying inside the surgetank increases to accelerate bubble release from the surface. Modeling of bubble release phenomenon is implemented considering this flow field.

To evaluate the swirl flow and structural influences correctly, 3D thermal-hydraulics simulation code (FLUENT) is used to simulate bubble behavior in the surgetank then modeling of bubble release ratio based on the simulation result is implemented. Bubble release ratio is formulated with dimensionless number representing characteristics of bubble and dipped plate (D/P) configuration, that is, formulating with dimensionless number (F_B/F_D), representing ratio of buoyancy and drag forces, and (I/D), ratio of the surgetank inner diameter D and gap I between surgetank wall and D/P.

Ratio of buoyancy force and drag force (F_B/F_D)

$$\frac{F_B}{F_D} = \frac{8rg}{3C_D V_{in}^{\ 2}} \cdot \frac{\rho_l - \rho_g}{\rho_l} \tag{5.5}$$

Note: ρ_l and ρ_g are density of fluid and gas respectively. C_D is drag coefficient and V_{in} is inlet flow velocity. Here, below is used for drag coefficient C_D based on the literature[8].

$$C_D = \max\left\{\min\left[\frac{24}{\mathrm{Re}}\left(1+0.15\,\mathrm{Re}^{0.687}\right), \frac{72}{\mathrm{Re}}\right], \frac{8}{3}\frac{Eo}{Eo+4}\right\} \tag{5.6}$$

Note: Re is Reynolds number and Eo is Eötvös number defined in below.

$$\mathrm{Re} = \frac{\rho_l V_{in} 2r}{\mu_l} \tag{5.7}$$

$$Eo = \frac{g(\rho_l - \rho_g)(2r)^2}{\sigma} \tag{5.8}$$

μ_l is liquid viscosity coefficient.

Ratio of gap I and inside diameter D (I/D)

If there is no D/P, $I=D$ is used. Thus I/D = 1 in such a case and the influence of D/P on bubble release ratio diminishes (see Eq. 5.10 below).

As shown in Fig 5.4, bubble release ratio f_{rel} based on the result of the numerical simulation is written as below.

$$f_{rel} = 1 - \exp(-450.5X^{1.1515391} - 0.035) \tag{5.9}$$

where

$$X = \left(\frac{F_B}{F_D}\right)\left(\frac{I}{D}\right)^{0.1} \tag{5.10}$$

Bubble release ratio in Eq. 5.9 is determined based on the simulation results in water-air system hence the applicability for mercury-helium system has to be confirmed. 3D numerical simulations in mercury-helium system are implemented and the results are compared to the bubble release ratio evaluated by Eq. 5.9 as shown in Fig. 5.5. Evaluation result by Eq. 5.9 generally reproduces simulation results thus bubble release ratio is considered applicable to the mercury-helium system.

As introduction of bubble release model in surgetank, four variables are introduced as new inputs (iflgstrel: selection of model, stVin: inflow velocity into the surgetank, dpI: Gap between D/P and surgetank wall, stD: inner diameter of surgetank).

To confirm the model performance in SYRENA code, two connected components are employed, bubbles are injected in upstream component and the bubble release model is activated in downstream component. Simulation conditions are similar to those in section 5.3. Two types of simulation with and without D/P (I = 0.002 (m)) are considered. Since bubble dissolution is not considered in the 3D numerical simulation, two cases are analyzed: one with no bubble dissolution, the other with zero inflow dissolved mol concentration. SYRENA simulation results (comparison of bubble release ratio through the surgetank outlet) of no D/P and I = 0.002 (m) are shown in Fig. 5.6 and 5.7. When bubble dissolution is neglected, bubble release ratio agrees with that evaluated by Eq. 3.9. On the other hand, when dissolved gas density is “0” in the surgetank, bubble dissolution becomes dominant and release ratio becomes less than 0.2. In the case with no bubble dissolution, SYRENA code provides the bubble release ratio coincident with Eq. 3.9 showing that the bubble release model works properly in SYRENA code.

5.5 Modeling of Bubble Coalescence and Accumulation

In a plenum structure, gas layer can be formed gradually by accumulation of the released bubble as shown in Fig. 5.8. To model this phenomenon new calculation function is developed.

Variation of gas accumulation volume (D_{glyr})

$$D_{glyr} = V_{rls} - V_{dssltn} \tag{5.11}$$

Note: V_{dssltn} (m^3) is volume of gas dissolution from the surface, V_{rls} (m^3) is gas release volume at the surface.

Gas accumulation volume (V_{glyr})

$$V_{glyr}^{n+1} = V_{glyr}^{n} + D_{glyr}^{n} \tag{5.12}$$

Note: if the gas accumulation volume is negative the gas accumulation volume is 0.

Modified bubble release coefficient (α'_i)

Bubble release coefficient varies with liquid volume. Therefore, modification is made with gas accumulation volume.

$$\alpha'_i = \alpha_i \times \frac{V_{\_ple}}{V_{\_ple} - V_{glyr}} \tag{5.13}$$

Note: $V_{\_ple}$ (m^3) is the volume of a plenum structure.

Liquid volume (V_{na})

$$V_{na} = V_{\_ple} - V_{glyr} \tag{5.14}$$

Note: when V_{na} becomes less than 0, the calculation is stopped.

Gas layer thickness (H_{glyr})

$$H_{glyr} = \frac{V_{glyr}}{S_{na}} \tag{5.15}$$

Note: S_{na} (m^2) is surface area.

Cover gas pressure (P_{lib_ple})

$$P_{lib\_ple} = \rho g(H_{\_ple} + H_{glyr}) \tag{5.16}$$

Note: $H_{\_ple}$ is height of a plenum, that is height from the baseline of static pressure calculation to the top of the plenum structure.

Due to introduction of gas accumulation model in a plenum structure, three new variables are utilized (iflgbubacc: model selection, v_ple: plenum volume, h_ple: plenum height).

To confirm the performance of the gas accumulation model in SYRENA code, bubble behavior is simulated in two connected components with bubble injection in upstream component and activated gas accumulation model in downstream component. Simulation conditions are basically same as section 5.3. Two simulation cases with different heat exchanger height ($H_{\_ple}$ = 1.0 and 15.0 (m)) are considered. In general, bubble release volume is larger than that of dissolved volume from liquid surface hence utilization of gas accumulation model alone (without carry-under model described in the next section) can make liquid volume in the plenum "0". As a matter of fact, in the case of $H_{\_ple}$ = 1.0 (m), gas accumulation volume linearly increase with time until liquid volume becomes zero as shown in Fig. 5.9. On the other hand, in the case of $H_{\_ple}$ = 15.0 (m), extremely increased gas pressure accelerate gas dissolution to make gas accumulation volume converge to the fixed value (1.2×10^{-7} (m^3)) as shown in Fig. 5.10. From these simulation results, gas accumulation is considered to be qualitatively reproduced by the developed model in heat exchanger.

5.6 Modeling of Carry-under (Gas Entrainment)

As implementation of modeling in section 5.5, gas layer is formed in a plenum structure due to bubble release. When the gas layer exists, it is postulated liquid jet injected vertically to the surface through the gas layer causes carry-under (gas entrainment). New calculation function below is developed to model carry-under.

Gas entrainment rate (Q_A)

Gas entrainment rate Q_A (m^3/s) is calculated with the equation below based on the reference literature[9].

$$Q_A = 0.04 F_{rj}^{\ 0.28} \left(\frac{H_{glyr}}{pleD_{in}} \right)^{0.4} Q_W \tag{5.17}$$

Note: $pleD_{in}$ (m) is inlet pipe diameter of a plenum, Q_W (m^3/s) is volumetric flow rate. Also, F_{rj} is Froude number and defined as below.

$$F_{rj} = \frac{pleV_{in}^{\ 2}}{g \times pleD_{in}} \tag{5.18}$$

Note: $pleV_{in}$ (m/s) is inlet flow velocity to a plenum.

Entrained gas volume (V_{QA})

$$V_{QA} = Q_A \Delta t \tag{5.19}$$

Gas accumulation volume （V_{glyr}）

$$V_{glyr}^{n+1} = V_{glyr}^{n} - V_{QA}^{n} \tag{5.20}$$

Note: in the case gas accumulation is negative, the volume is “0”.

Entrained bubble number density (N_{bi_QA})

Radius of the entrained bubble is given as input and bubble number density added to the designated bubble group is calculated with the equation below.

$$N_{bi\_QA} = \frac{V_{QA}}{\frac{4}{3}\pi r_{QA}^3} \frac{1}{V_{na}} \tag{5.21}$$

Note: r_{QA} (m) is radius of the entrained bubble.

As introduction of carry-under model in a plenum, four variables are introduced as new inputs (iflgcrryudr: model selection, pleVin: inlet flow velocity, pleDin: inlet pipe diameter, rcrryudr: entrained bubble radius).

To confirm the performance of carry-under model in SYRENA code, simulation is implemented by arranging two connected components with bubble injection in upstream component and carry-under model activation in downstream component. Basic simulation conditions are same as section 5.3. Note, initial gas accumulation volume at the downstream component is 0.1 (m^3). In this simulation, the carry-under model is utilized individually and bubble release from the liquid surface is not added to the gas layer. As a matter of fact, accumulated gas volume decreases monotonically with time as shown in Fig. 5.11, showing the carry-under model operate correctly.

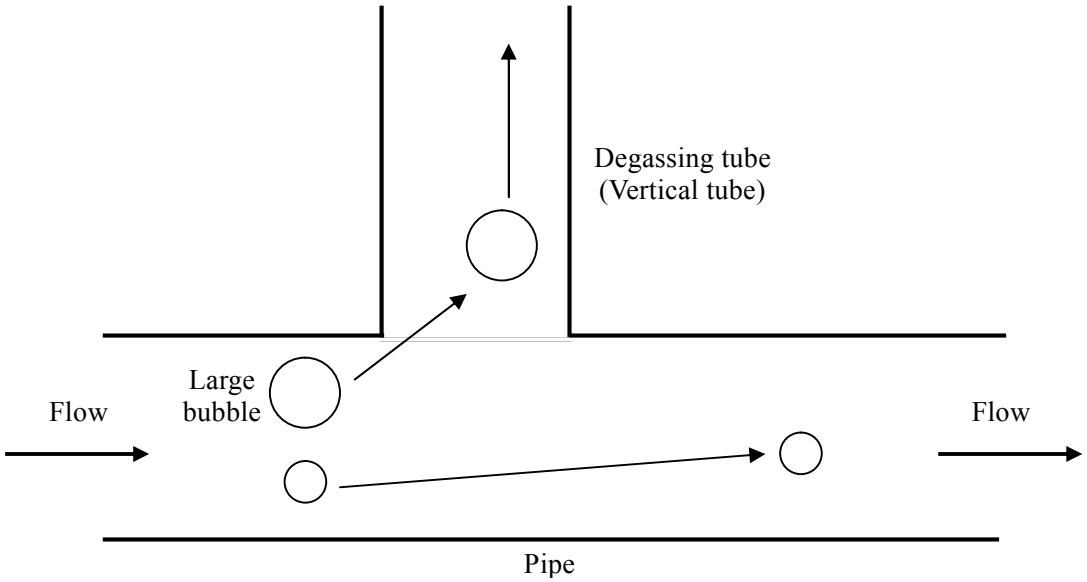

Fig.5.1 Large bubble release through degassing tube

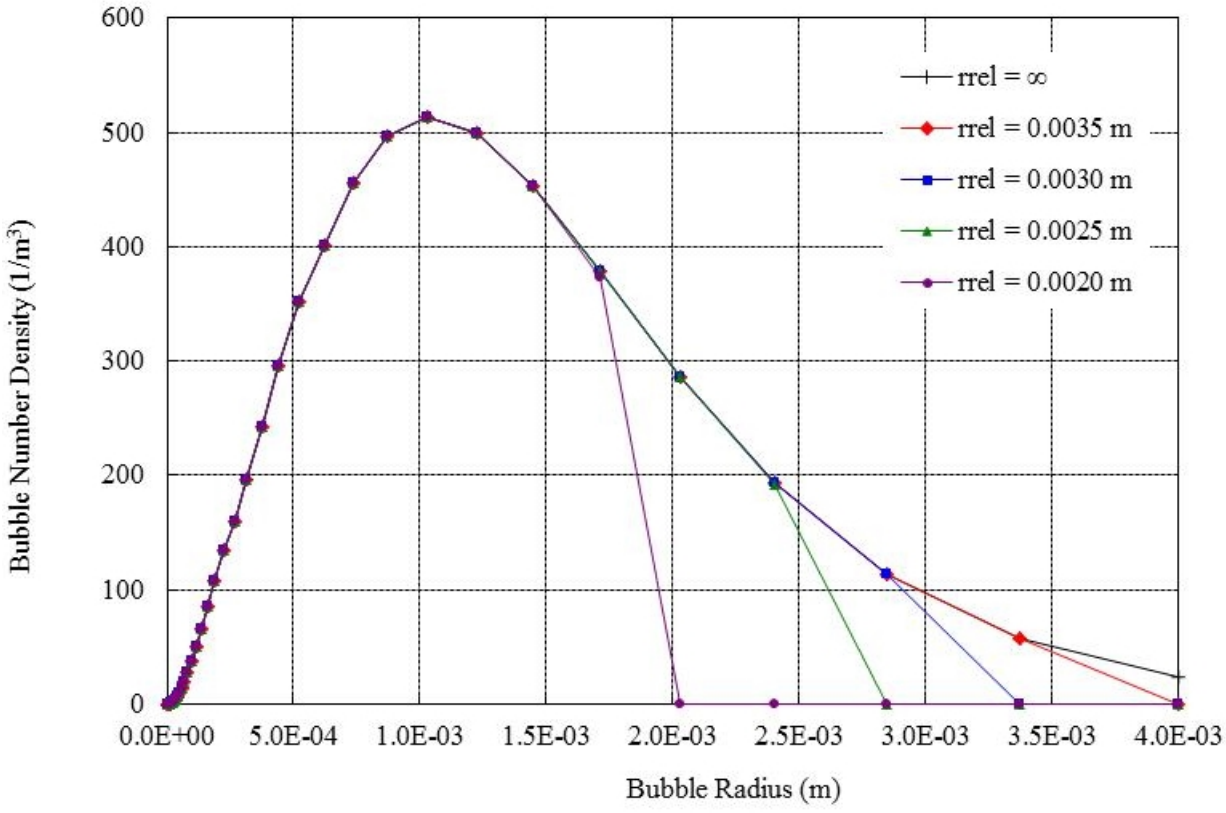

Fig.5.2 Influence of large bubble release model on bubble number density distribution

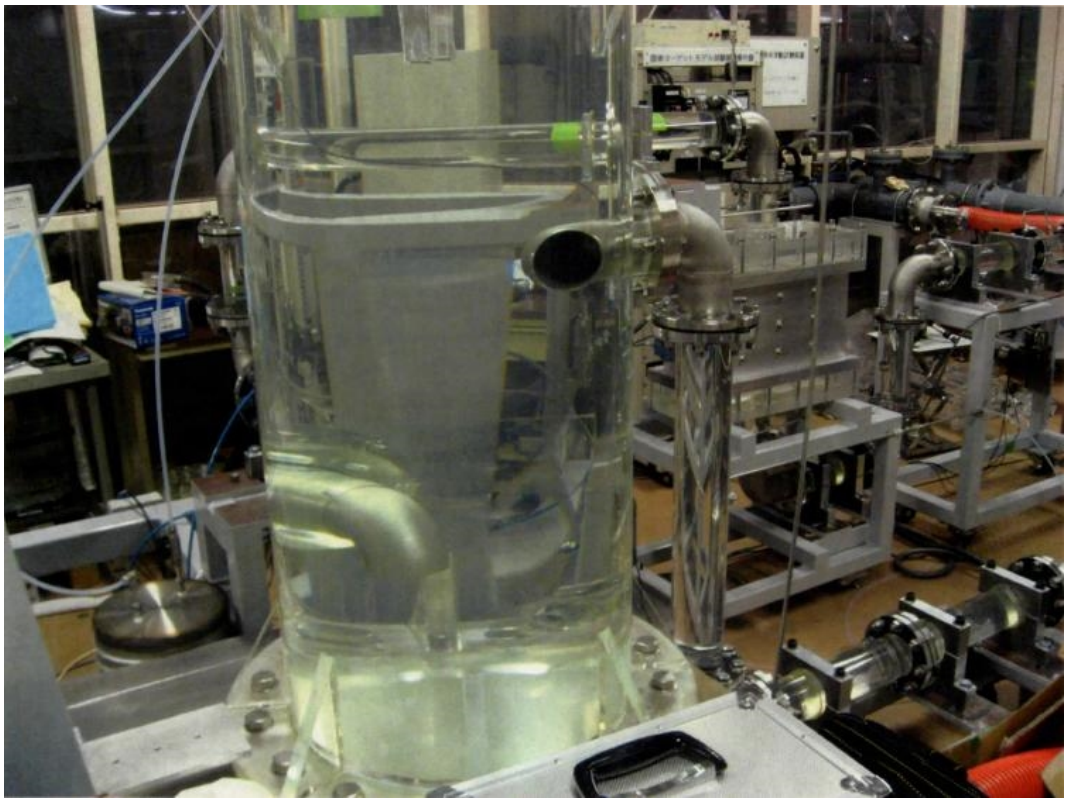

Fig.5.3　Example of surgetank

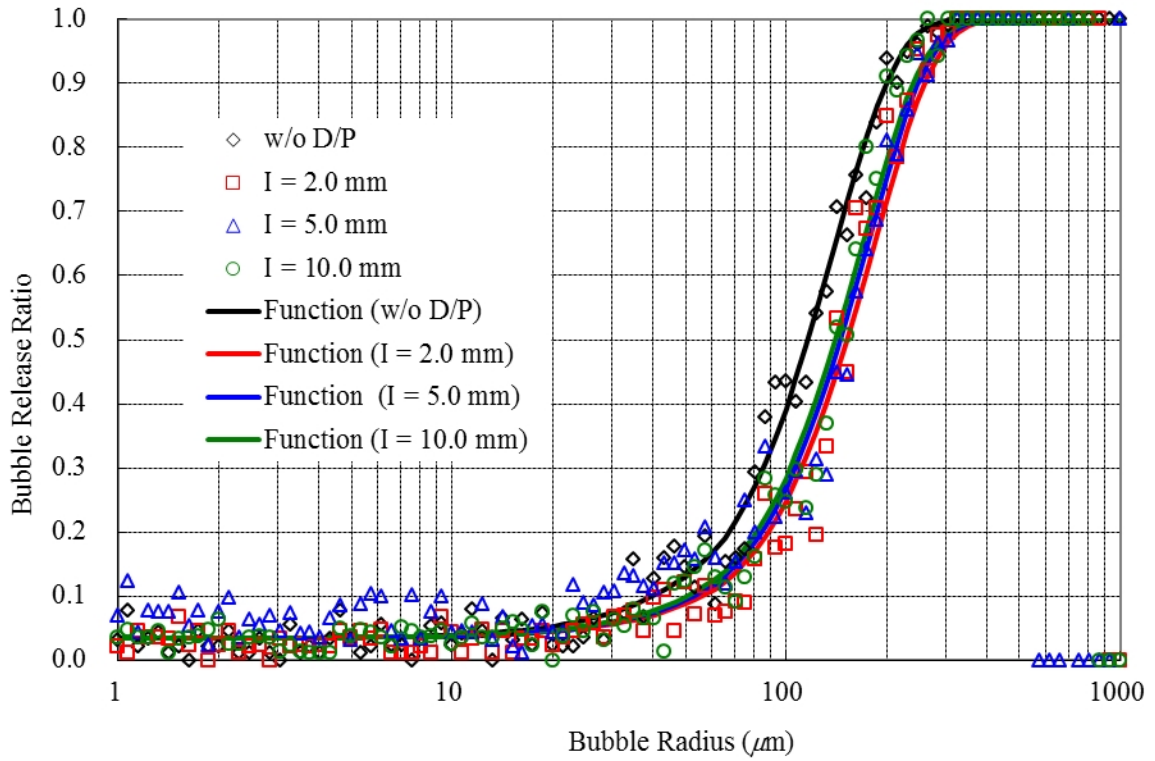

Fig.5.4 Bubble release ratio in water-air system

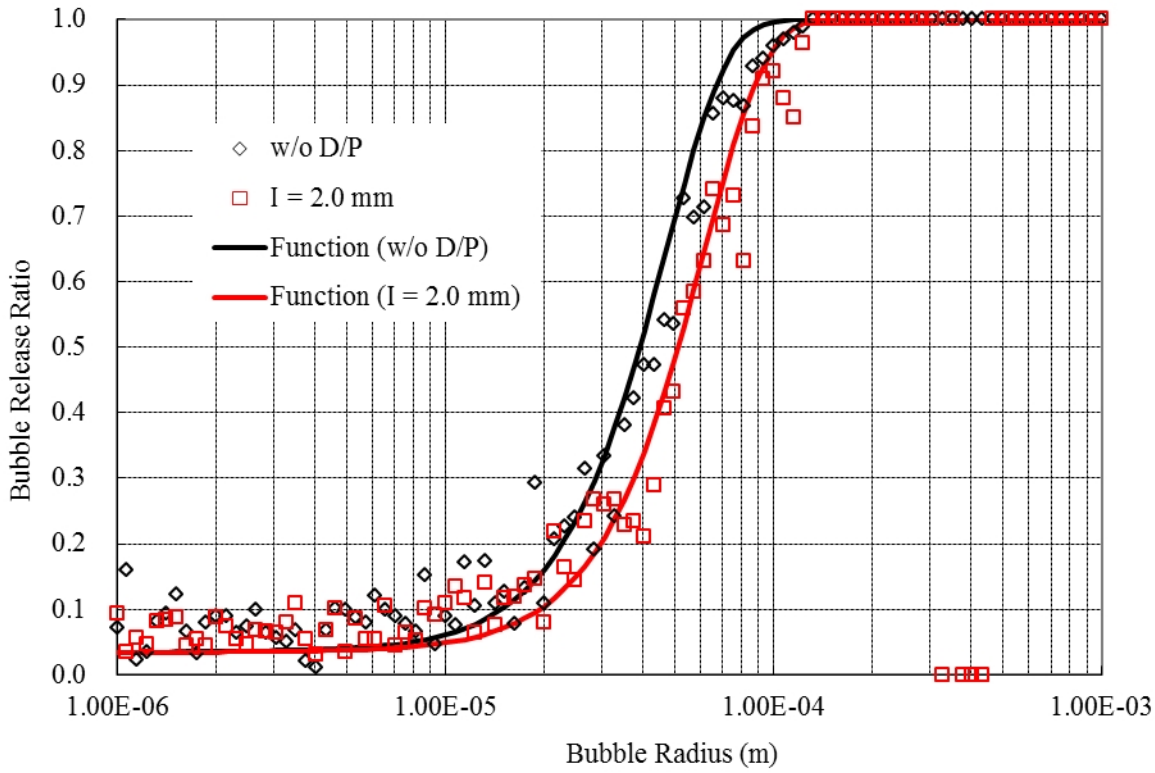

Fig.5.5 Bubble release ratio in mercury-helium system

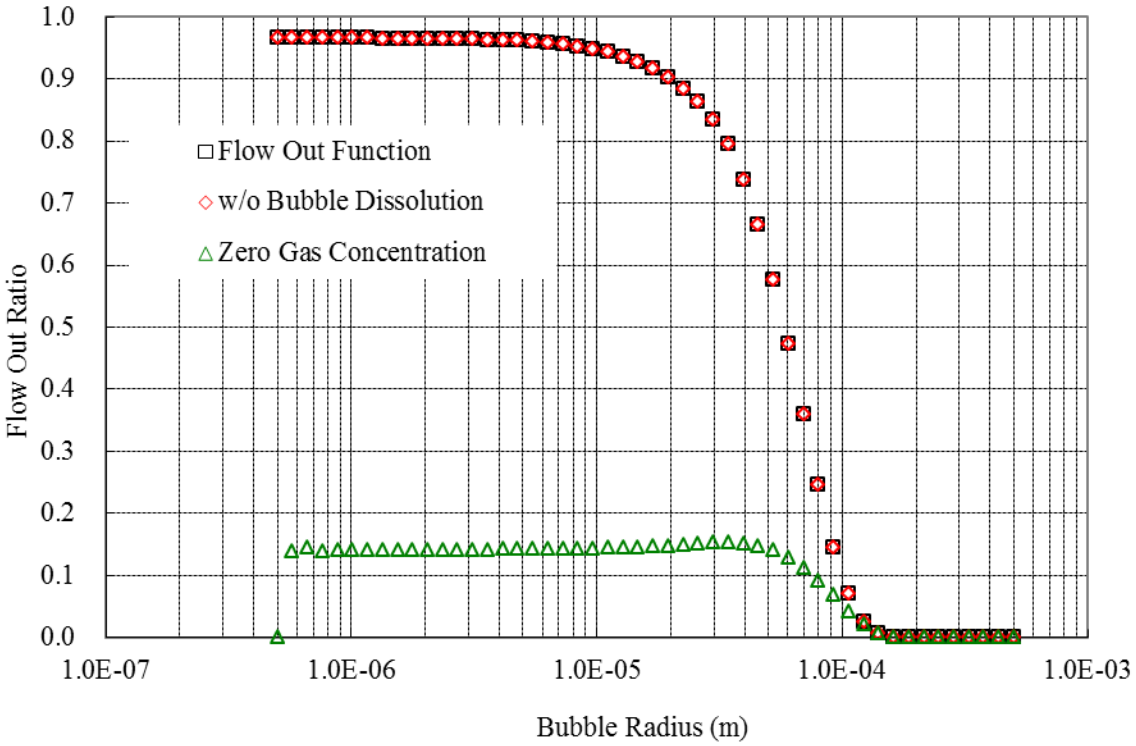

Fig.5.6 Bubble release ratio through surgetank outlet (w/o D/P)

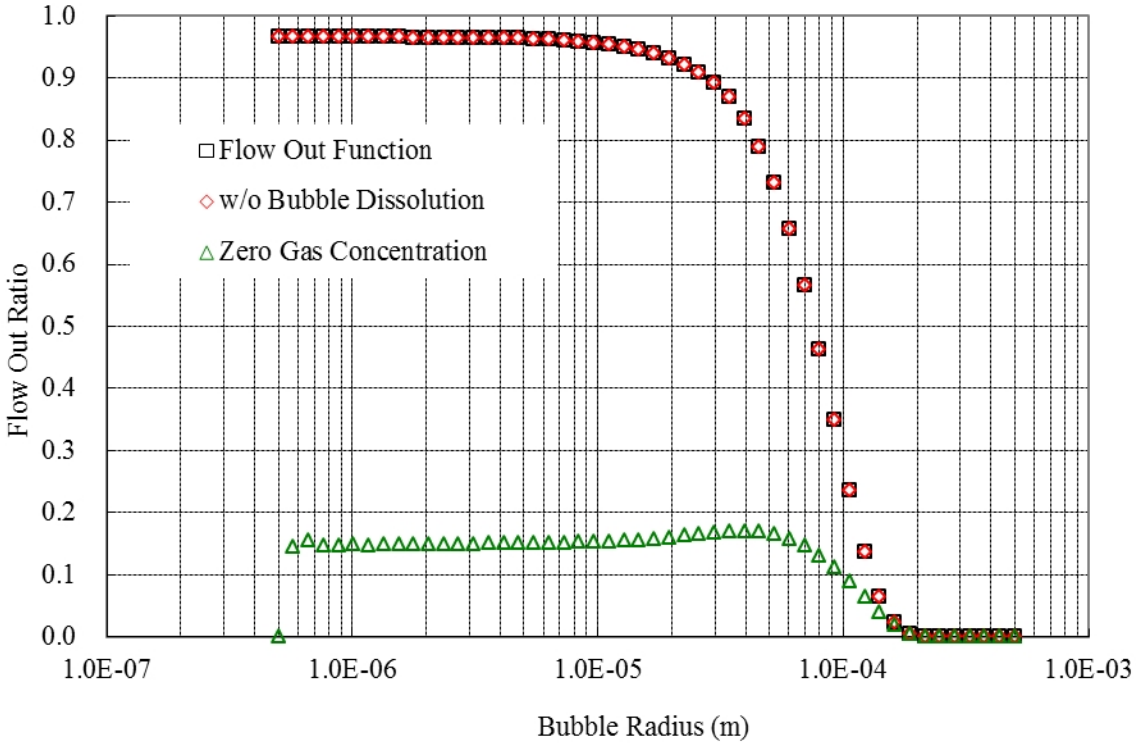

Fig.5.7 Bubble release ratio through surgetank outlet (D/P with 2.0 (mm) gap)

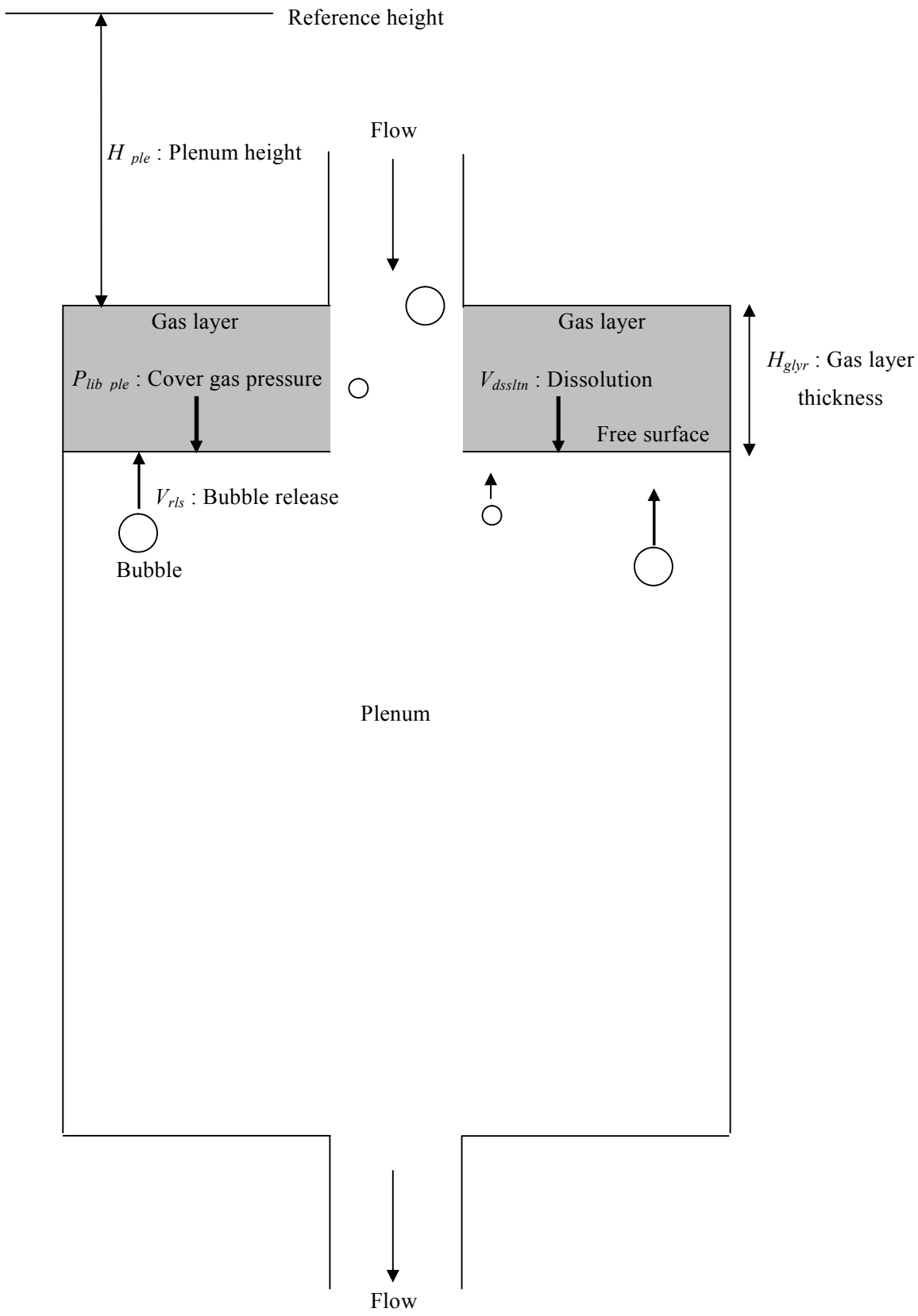

Fig.5.8 Bubble behavior in plenum

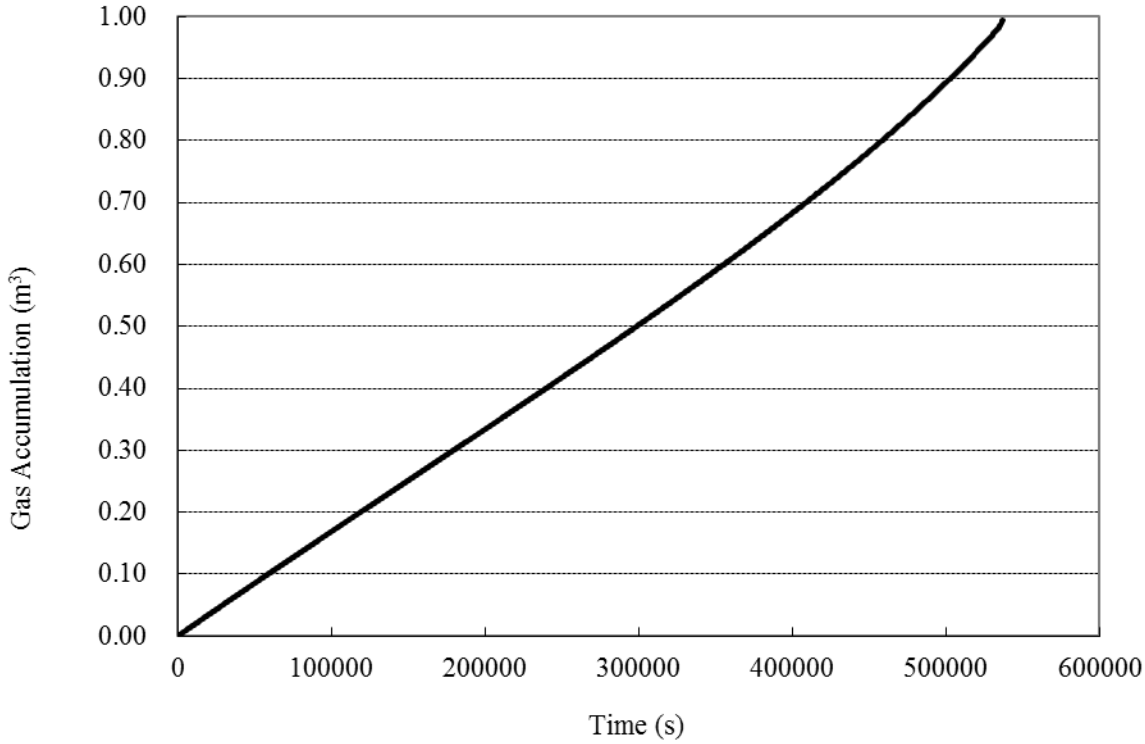

Fig.5.9 Time variation of gas accumulation volume (1.0 (m) height)

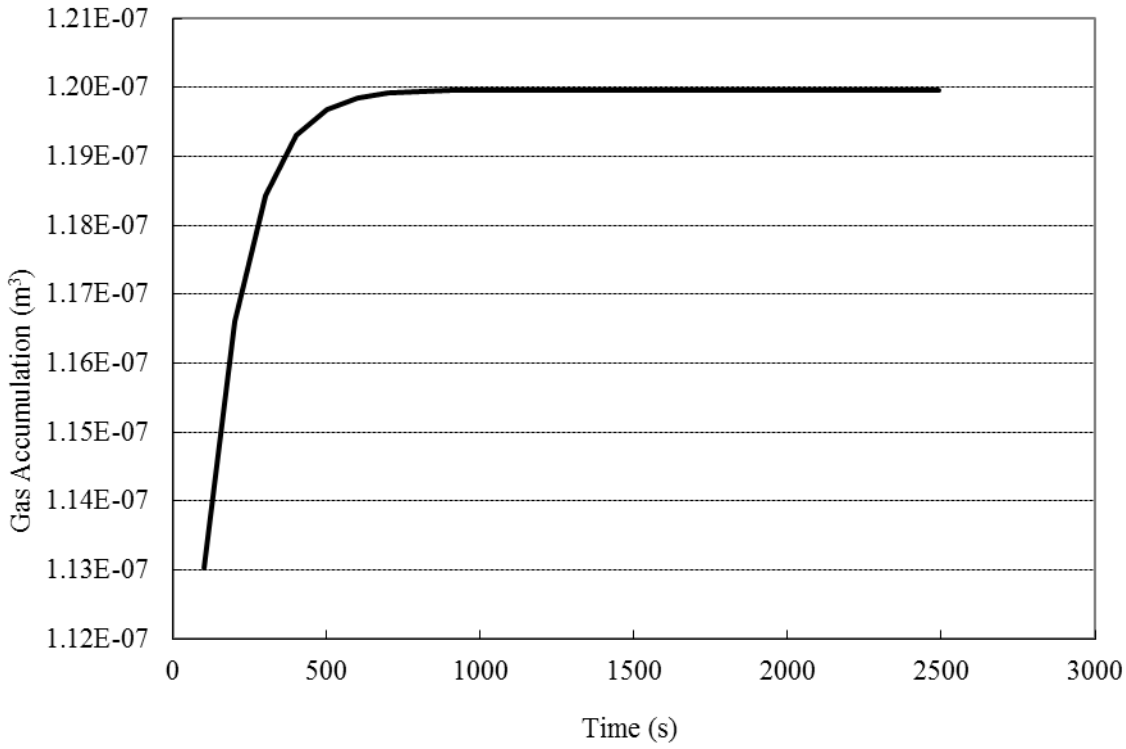

Fig.5.10 Time variation of gas accumulation volume (15.0 (m) height)

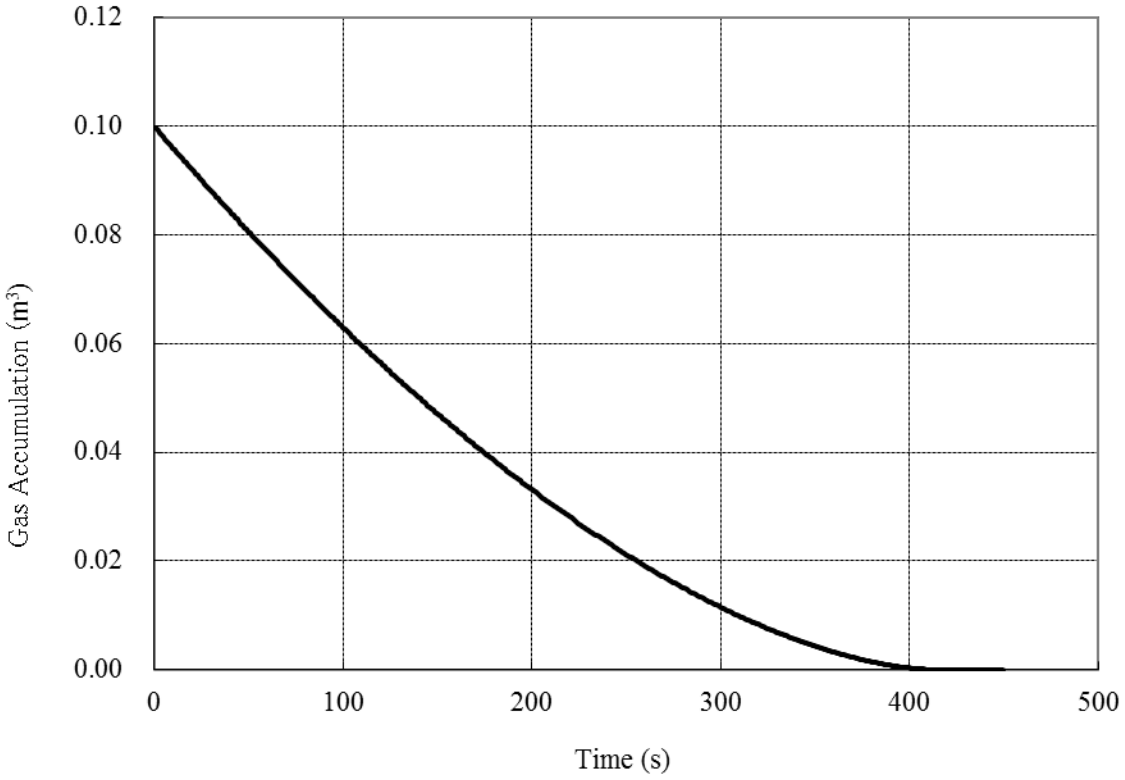

Fig.5.11 Time variation of gas accumulation volume with carry-under model

6. Concluding Remarks

Knowledge below was accumulated by developing the models in SYRENA code and applying the improved models to the numerical simulations to evaluate bubble and dissolved gas behavior of inert gas (Ar, He) in primary cooling system of sodium cooled fast reactor.

(1) Improvement of models in SYRENA code

Several code modifications, i.e. explicitly discretization to the conservation equation of bubble mol count, initialization of nucleation calculation, saturated temperature calculation in sodium, pressure calculation in IHX and calculation of dissolved mol concentration at mixing point, are achieved and correct calculation of bubble behavior (mol conservation) was confirmed.

(2) Simulation of JSFR system

Bubble/ dissolved gas behaviors in each component of JSFR are simulated and influence of bubble source is evaluated. In addition, behavioral difference between Ar gas and He gas are confirmed.

(3) New model development

Liquid property of mercury, open loop calculation method, large bubble release model, bubble release model in surge tank, gas accumulation model and carry-under (gas entrainment) model in a plenum are developed and introduced into SYRENA code. Applicability confirmations of each model were implemented to show bubble behavior calculation in each component is appropriate.

References

1) J. L. Berton : “VIBUL, Un Modele de Calcul de la Vie des Bulles en Reacteur”, Note Technique, CEA/Cadarache (1991).
2) A. Yamaguchi and A. Hashimoto : “A computational model for dissolved gas and bubble behavior in the primary coolant system of sodium-cooled fast reactor”, Proceedings of the 11th International Topical Meeting on Nuclear Reactor Thermal-Hydraulics, Avignon, France, Oct. 2-6 (2005).
3) E. Tatsumi, T. Takata, A. Yamaguchi : “Modeling and Quantification of Nucleation, Dissolution and Transportation of Bubbles in Primary Coolant System of Sodium Fast Reactor”, Proceedings of the 15th International Conference on Nuclear Engineering, Nagoya, Japan, Apr. 22-26 (2007).
4) A. Yamaguchi, E. Tatsumi, T. Takata, K. Ito, H. Ohshima, H. Kamide, J. Sakakibara : “Gas entrainment allowance level at free surface and gas dynamic behavior of sodium-cooled fast reactor”, Nuclear Engineering and Design, 241(5) (2011), pp. 1627-1635.
5) The Japan Society of Mechanical Engineers, “JSME Data Book: Heat Transfer 5th Edition”, ISBN 978-4-88898-184-2 (2009). (in Japanese)
6) S. Hasegawa, T. Naoe, M. Futakawa : “Solubility of helium in mercury for bubbling technology of the spallation neutron mercury target”, Journal of Nuclear Materials, 398 (2010), pp. 189-192.
7) E. L. Reed, J. J. Droher : “Solubility and Diffusivity of Inert Gases in Liquid Sodium, Potassium, and NaK”, Liquid Metal Engineering Center. Report LMEC-69-36 Issued: Jan. 31 (1970).
8) M. Akiyama, M. Aritomi, “Advanced Numerical Analysis of Two-Phase Flow Dynamics – Multi-Dimensional Flow Analysis –”, CORONA Publishing Co., LTD (2002). (in Japanese)
9) K. Bin, Andrzej : “Gas Entrainment by Plunging Liquid Jets”, Chemical Engineering Science, 48(21) (1993), pp. 3585-3630.

国際単位系（SI）

表１．SI 基本単位

基本量	SI 基本単位	
	名称	記号
長さ	メートル	m
質量	キログラム	kg
時間	秒	s
電流	アンペア	A
熱力学温度	ケルビン	K
物質量	モル	mol
光度	カンデラ	cd

表２．基本単位を用いて表されるSI組立単位の例

組立量	SI 基本単位	
	名称	記号
面積	平方メートル	m^2
体積	立法メートル	m^3
速さ，速度	メートル毎秒	m/s
加速度	メートル毎秒毎秒	m/s^2
波数	毎メートル	m^{-1}
密度，質量密度	キログラム毎立方メートル	kg/m^3
面積密度	キログラム毎平方メートル	kg/m^2
比体積	立方メートル毎キログラム	m^3/kg
電流密度	アンペア毎平方メートル	A/m^2
磁界の強さ	アンペア毎メートル	A/m
量濃度(a)，濃度	モル毎立方メートル	mol/m^3
質量濃度	キログラム毎立法メートル	kg/m^3
輝度	カンデラ毎平方メートル	cd/m^2
屈折率(b)	（数字の） 1	1
比透磁率(b)	（数字の） 1	1

(a) 量濃度（amount concentration）は臨床化学の分野では物質濃度（substance concentration）ともよばれる。
(b) これらは無次元量あるいは次元１をもつ量であるが、そのことを表す単位記号である数字の１は通常は表記しない。

表３．固有の名称と記号で表されるSI組立単位

組立量	SI 組立単位			
	名称	記号	他のSI単位による表し方	SI基本単位による表し方
平面角	ラジアン(b)	rad	1 (b)	m/m
立体角	ステラジアン(b)	sr(c)	1 (b)	m^2/m^2
周波数	ヘルツ(d)	Hz		s^{-1}
力	ニュートン	N		m kg s^{-2}
圧力，応力	パスカル	Pa	N/m^2	m^{-1} kg s^{-2}
エネルギー，仕事，熱量	ジュール	J	N m	m^2 kg s^{-2}
仕事率，工率，放射束	ワット	W	J/s	m^2 kg s^{-3}
電荷，電気量	クーロン	C		s A
電位差（電圧），起電力	ボルト	V	W/A	m^2 kg s^{-3} A^{-1}
静電容量	ファラド	F	C/V	m^{-2} kg^{-1} s^4 A^2
電気抵抗	オーム	Ω	V/A	m^2 kg s^{-3} A^{-2}
コンダクタンス	ジーメンス	S	A/V	m^{-2} kg^{-1} s^3 A^2
磁束	ウエーバ	Wb	Vs	m^2 kg s^{-2} A^{-1}
磁束密度	テスラ	T	Wb/m^2	kg s^{-2} A^{-1}
インダクタンス	ヘンリー	H	Wb/A	m^2 kg s^{-2} A^{-2}
セルシウス温度	セルシウス度(e)	℃		K
光束	ルーメン	lm	cd sr(c)	cd
照度	ルクス	lx	lm/m^2	m^{-2} cd
放射性核種の放射能(f)	ベクレル(d)	Bq		s^{-1}
吸収線量，比エネルギー分与，カーマ	グレイ	Gy	J/kg	m^2 s^{-2}
線量当量，周辺線量当量，方向性線量当量，個人線量当量	シーベルト(g)	Sv	J/kg	m^2 s^{-2}
酸素活性	カタール	kat		s^{-1} mol

(a)SI接頭語は固有の名称と記号を持つ組立単位と組み合わせても使用できる。しかし接頭語を付した単位はもはやコヒーレントではない。
(b)ラジアンとステラジアンは数字の１に対する単位の特別な名称で、量についての情報をつたえるために使われる。実際には、使用する時には記号rad及びsrが用いられるが、習慣として組立単位としての記号である数字の１は明示されない。
(c)測光学ではステラジアンという名称と記号srを単位の表し方の中に、そのまま維持している。
(d)ヘルツは周期現象についてのみ、ベクレルは放射性核種の統計的過程についてのみ使用される。
(e)セルシウス度はケルビンの特別な名称で、セルシウス温度を表すために使用される。セルシウス度とケルビンの単位の大きさは同一である。したがって、温度差や温度間隔を表す数値はどちらの単位で表しても同じである。
(f)放射性核種の放射能（activity referred to a radionuclide）は、しばしば誤った用語で"radioactivity"と記される。
(g)単位シーベルト（PV,2002,70,205）についてはCIPM勧告2（CI-2002）を参照。

表４．単位の中に固有の名称と記号を含むSI組立単位の例

組立量	SI 組立単位		
	名称	記号	SI 基本単位による表し方
粘度	パスカル秒	Pa s	m^{-1} kg s^{-1}
力のモーメント	ニュートンメートル	N m	m^2 kg s^{-2}
表面張力	ニュートン毎メートル	N/m	kg s^{-2}
角速度	ラジアン毎秒	rad/s	m m^{-1} s^{-1}=s^{-1}
角加速度	ラジアン毎秒毎秒	rad/s^2	m m^{-1} s^{-2}=s^{-2}
熱流密度，放射照度	ワット毎平方メートル	W/m^2	kg s^{-3}
熱容量，エントロピー	ジュール毎ケルビン	J/K	m^2 kg s^{-2} K^{-1}
比熱容量，比エントロピー	ジュール毎キログラム毎ケルビン	J/(kg K)	m^2 s^{-2} K^{-1}
比エネルギー	ジュール毎キログラム	J/kg	m^2 s^{-2}
熱伝導率	ワット毎メートル毎ケルビン	W/(m K)	m kg s^{-3} K^{-1}
体積エネルギー	ジュール毎立方メートル	J/m^3	m^{-1} kg s^{-2}
電界の強さ	ボルト毎メートル	V/m	m kg s^{-3} A^{-1}
電荷密度	クーロン毎立方メートル	C/m^3	m^{-3} sA
表面電荷	クーロン毎平方メートル	C/m^2	m^{-2} sA
電束密度，電気変位	クーロン毎平方メートル	C/m^2	m^{-2} sA
誘電率	ファラド毎メートル	F/m	m^{-3} kg^{-1} s^4 A^2
透磁率	ヘンリー毎メートル	H/m	m kg s^{-2} A^{-2}
モルエネルギー	ジュール毎モル	J/mol	m^2 kg s^{-2} mol^{-1}
モルエントロピー，モル熱容量	ジュール毎モル毎ケルビン	J/(mol K)	m^2 kg s^{-2} K^{-1} mol^{-1}
照射線量（X線及びγ線）	クーロン毎キログラム	C/kg	kg^{-1} sA
吸収線量率	グレイ毎秒	Gy/s	m^2 s^{-3}
放射強度	ワット毎ステラジアン	W/sr	m^4 m^{-2} kg s^{-3}=m^2 kg s^{-3}
放射輝度	ワット毎平方メートル毎ステラジアン	$W/(m^2$ sr)	m^2 m^{-2} kg s^{-3}=kg s^{-3}
酵素活性濃度	カタール毎立方メートル	kat/m^3	m^{-3} s^{-1} mol

表５．SI 接頭語

乗数	接頭語	記号	乗数	接頭語	記号
10^{24}	ヨタ	Y	10^{-1}	デシ	d
10^{21}	ゼタ	Z	10^{-2}	センチ	c
10^{18}	エクサ	E	10^{-3}	ミリ	m
10^{15}	ペタ	P	10^{-6}	マイクロ	μ
10^{12}	テラ	T	10^{-9}	ナノ	n
10^{9}	ギガ	G	10^{-12}	ピコ	p
10^{6}	メガ	M	10^{-15}	フェムト	f
10^{3}	キロ	k	10^{-18}	アト	a
10^{2}	ヘクト	h	10^{-21}	ゼプト	z
10^{1}	デカ	da	10^{-24}	ヨクト	y

表６．SIに属さないが、SIと併用される単位

名称	記号	SI 単位による値
分	min	1 min=60s
時	h	1h =60 min=3600 s
日	d	1 d=24 h=86 400 s
度	°	1°=(π/180) rad
分	’	1’=(1/60)°=(π/10800) rad
秒	”	1”=(1/60)’=(π/648000) rad
ヘクタール	ha	$1ha=1hm^2=10^4m^2$
リットル	L, l	$1L=1l=1dm^3=10^3cm^3=10^{-3}m^3$
トン	t	$1t=10^3$ kg

表７．SIに属さないが、SIと併用される単位で、SI単位で表される数値が実験的に得られるもの

名称	記号	SI 単位で表される数値
電子ボルト	eV	$1eV=1.602\ 176\ 53(14)\times10^{-19}J$
ダルトン	Da	$1Da=1.660\ 538\ 86(28)\times10^{-27}kg$
統一原子質量単位	u	1u=1 Da
天文単位	ua	$1ua=1.495\ 978\ 706\ 91(6)\times10^{11}m$

表８．SIに属さないが、SIと併用されるその他の単位

名称	記号	SI 単位で表される数値
バール	bar	1 bar=0.1MPa=100kPa=10^5Pa
水銀柱ミリメートル	mmHg	1mmHg=133.322Pa
オングストローム	Å	1 Å=0.1nm=100pm=10^{-10}m
海里	M	1 M=1852m
バーン	b	$1\ b=100fm^2=(10^{-12}cm)2=10^{-28}m^2$
ノット	kn	1 kn=(1852/3600)m/s
ネーパ	Np	SI単位との数値的な関係は、対数量の定義に依存。
ベル	B	
デシベル	dB	

表９．固有の名称をもつCGS組立単位

名称	記号	SI 単位で表される数値
エルグ	erg	$1\ erg=10^{-7}$ J
ダイン	dyn	$1\ dyn=10^{-5}$N
ポアズ	P	1 P=1 dyn s cm^{-2}=0.1Pa s
ストークス	St	1 St =$1cm^2$ s^{-1}=$10^{-4}m^2$ s^{-1}
スチルブ	sb	1 sb =1cd cm^{-2}=10^4cd m^{-2}
フォト	ph	1 ph=1cd sr cm^{-2} 10^4lx
ガル	Gal	1 Gal =1cm s^{-2}=$10^{-2}ms^{-2}$
マクスウェル	Mx	1 Mx = 1G cm^2=10^{-8}Wb
ガウス	G	1 G =1Mx cm^{-2} =10^{-4}T
エルステッド(c)	Oe	1 Oe≙ $(10^3/4\pi)$A m^{-1}

(c) ３元系のCGS単位系とSIでは直接比較できないため、等号「 ≙ 」は対応関係を示すものである。

表10．SIに属さないその他の単位の例

名称	記号	SI 単位で表される数値
キュリー	Ci	$1\ Ci=3.7\times10^{10}Bq$
レントゲン	R	$1\ R = 2.58\times10^{-4}C/kg$
ラド	rad	$1\ rad=1cGy=10^{-2}Gy$
レム	rem	$1\ rem=1\ cSv=10^{-2}Sv$
ガンマ	γ	1 γ =1 nT=10-9T
フェルミ		1フェルミ=1 fm=10-15m
メートル系カラット		1メートル系カラット = 200 mg = 2×10-4kg
トル	Torr	1 Torr = (101 325/760) Pa
標準大気圧	atm	1 atm = 101 325 Pa
カロリー	cal	1cal=4.1858J（「15℃」カロリー），4.1868J（「IT」カロリー）4.184J（「熱化学」カロリー）
ミクロン	μ	1 μ =1μm=10^{-6}m

（第8版，2006年改訂）